5a

Filled Carbon Nanotubes: (X@CNTs)

Jeremy Sloan[1] *and Marc Monthioux*[2]
[1]*Dept. of Physics, University of Warwick, UK*
[2]*CEMES, CNRS, University of Toulouse, France*

5a.1 Introduction

Whilst fullerene and related materials are the most inserted molecules in carbon nanotubes (CNTs), other molecular species including Zn-diphenylporphyrin (i.e. Zn-DPP) [1], *ortho*-carborane [2,3], metallocenes [4,5], octasiloxane [6] and squarylium dye [7], among others have been encapsulated within either single-, double- or multiple walled carbon nanotubes (SWCNTs, DWCNTs and MWCNTs, respectively) and directly imaged by either high resolution transmission electron microscopy (HRTEM) or related techniques. In tandem with these studies, one-dimensional (1D) nanowires of a wide variety of materials including multiplets of polymeric iodine chains [8,9], pure metals [10–15], metal oxides [16–18], metal carbides [19–21], $2 \times 2 \times \infty$ or $3 \times 3 \times \infty$ atomic layer thick KI crystals [22,23], polyhedral chains of lanthanide trihalides [24,25], twisted 1D Co_2I_4 double chains with tetrahedral Co^{2+} coordination [26], a new trigonal tubular form of HgTe [27], reduced coordination polymorphs of PbI_2 [28], alloys [29,30] and semiconductor liquid-metal heterojunctions [31] have also been encapsulated within CNTs. Further, ab initio theory has been used to either predict or explain the formation of some of the above and several other encapsulated species, for example, silver atoms [32], hydrogen molecules [33] and ice crystals [34,35].

Carbon Meta-Nanotubes: Synthesis, Properties and Applications, First Edition. Edited by Marc Monthioux.

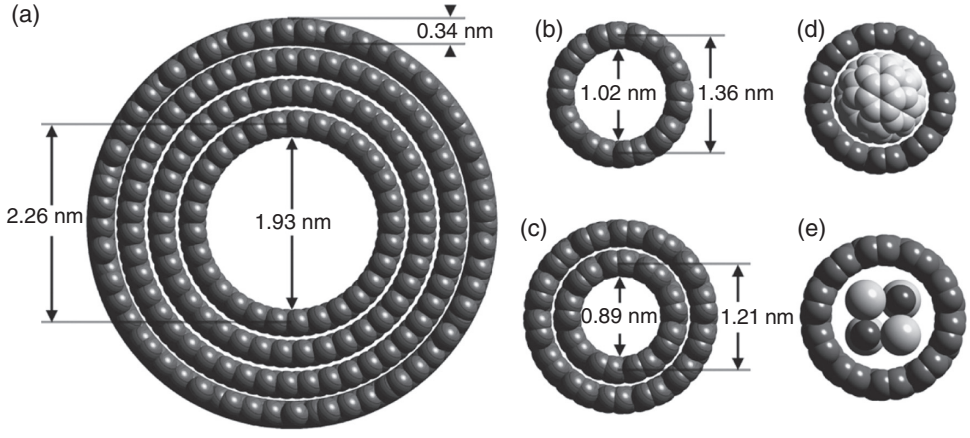

Figure 5a.1 *Structure models (a) a (29,0)@(38,0)@(47,0)@(48,13) MWCNT; (b) a (10,10) SWCNT; (c) a (9,9)@(14,14) DWCNT; (d) a C_{60} molecule (white spheres) inside a (10,10) SWCNT (dark spheres); (e) a 2 × 2 KI crystal inside a (10,10) SWCNT (white spheres = iodine, black spheres = potassium).*

The extent to which a nanotube can accommodate a species may be considered, to a first approximation, to be a function of the overall diameter of the encapsulating nanotube, partly specified by the (*n*,*m*) structural conformation of the nanotube, which dictates the nanotube diameter [36] and by the twofold contribution of the 0.17 nm van der Waals radii of the wall carbons which constrains the internal volume still further [37]. In Figure 5a.1, we can see how these factors influence the available free internal cross-section of a selection of nanotubes, including a MWCNT, a SWCNT and a DWCNT. With regard to the size of a species which may be accommodated, this will be specified by the internal diameter of the innermost SWCNT of a multi-walled nanotube (i.e. as in the case of a MWCNT or a DWCNT) or of the SWCNT itself (which consists of one graphene tubule only). Thus the MWCNT in Figure 5a.1(a) has an internal cylinder of 1.93 nm in diameter specified by the innermost (29,0) SWCNT, while the corresponding dimension for the (10,10) SWCNT in Figure 5a.1(b) is just 1.02 nm. The inner tube in the DWCNT specified in Figure 5a.1(c) is a (9,9) SWCNT which has a corresponding internal diameter of 0.89 nm which is narrower than for the (10,10) SWCNT in Figure 5a.1(b). The size of the inner surfaces of the narrower SWNTs and DWNTs correspond to the external dimensions either of single molecules, as exemplified by the encapsulation C_{60} molecule in Figure 5a.1(d) or of integral numbers of atomic layers of crystalline materials, as exemplified by the encapsulated 2 × 2 KI crystal shown in Figure 5a.1(e).

The dimensions of the nanotubes specified in Figure 5a.1 (and, by extension, nanotubes of both larger and smaller sizes) determine the available space within a nanotube for encapsulation although this does not tell the whole story. Beyond the simplistic consideration that a minimal inner diameter for the nanotube to fill could be merely required [38], we also have to consider the 'wetability' of the interior surface of the nanotube [39,40] in terms of the carbon and also in terms of the surface tension properties of the introduced liquid or solution and also whether or not the nanotubes are open at one or both ends (or contain sufficiently large voids in the graphene walls forming the nanotubes to permit

filling). If we are considering a species introduced from the vapour phase, we need to think in terms of the diffusion characteristics of the gaseous species and the relative permeability of the nanotube in terms of wall and tip holes. In order to be more rigorous, we may also need to consider more subtle structural features of the encapsulating nanotubes, such as: (i) defects which may take the form of gross structural defects, for example, bends and internal caps; (ii) the effective pitch of the nanotube, specified by the relative (*n*,*m*) helical conformation of a particular nanotube; (iii) the effect of relative rigidity on the nanotube when the tubule comprises two or more shells, which can sometimes cause differences in crystallization behaviour; (iv) the possible influence of the wall corrugation on encapsulate behaviour which may play some role in terms of fixing species into place or providing a register which can either assist or inhibit crystallization (i.e. in the Burger's vector sense); (v) the physical size and shape of the filling material, especially if it is molecular; and finally (vi) probably the most significant interaction, that is, the electronic interaction between nanotube and filling which can be defined either in terms of a mutual interaction (i.e. between either a semiconducting or metallic nanotube and a filling with different electronic properties) or in terms of the effect that confinement can have on a particular material. Both can potentially cause significant effects on the band structure of the nanotube itself or on the corresponding electronic structure of the filling material as well.

The desire to synthesize meta-nanotubes consisting of encapsulated materials within carbon nanotubes (which we shall abbreviate here 'X@CNT' where X is the introduced material and CNT is the collective term for all kinds of carbon nanotubes) consists of a multiplicity of motivations, including, among others, (i) to 'see' and study low dimensional crystals, single molecules and even functional groups attached to the latter, protected from the environment by the carbon sheath, with their mobility hindered by the interaction with it; (ii) to observe the formation of low dimensional crystal structures and, in so doing, occasionally observe new ones; (iii) to modify the physical properties of the encapsulating nanotubes and of the encapsulated materials; (iv) to use the obtained species as a means for both testing and exploiting the very latest in nanoscale characterization methodologies; (v) to correlate structural and electronic behaviour on materials formed on such a scale as to be tractable to the most rigorous computational methods (including both molecular dynamics (MD) and density functional theory (DFT)); and, ultimately, (vi) to satisfy that most fundamental of solid state science objectives, in other words to synthesize useful new materials or devices with useful applications on the nanometre scale. The goal of this chapter is therefore to evaluate the progress made so far in realising these objectives and perhaps give some idea of the work still remaining to be done although hopefully the reader will be pleasantly surprised with the amount of progress that has already been made.

5a.2 Synthesis of X@CNTs

5a.2.1 A Glimpse at the Past

The story of filled nanotubes started in 1993, where four papers were published that reported filling of MWCNTs with various metals and compounds (PbO_x [16], Y_3C and TiC [19] Bi_2O_5 [41] and Ni [42]) in attempts to obtain encapsulated inorganic nanowires.

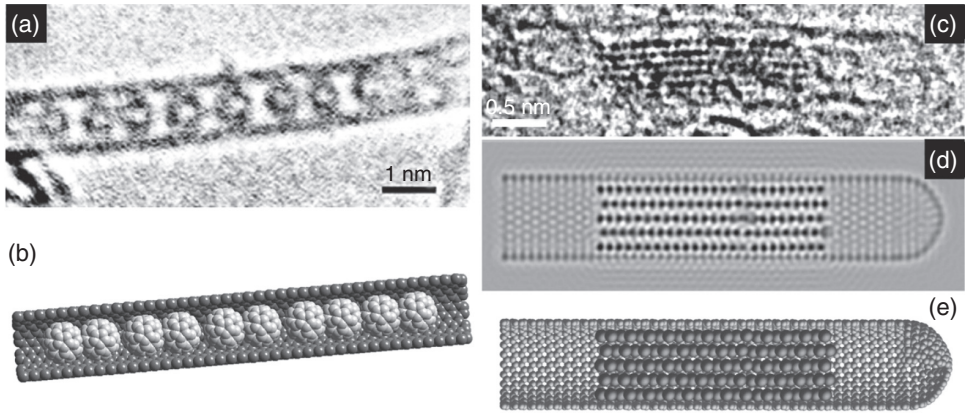

Figure 5a.2 *(a) The first HRTEM image of a C_{60}@SWCNT (peapod) nanocomposite (reproduced with permission from [46] Copyright (1998) Macmillan Publishers Ltd). (b) Corresponding structure model. (c) The first example of a metal@SWCNT (reprinted from [10] Copyright (1998) The Royal Society of Chemistry); in this case, the metal is Ru and was initially introduced as $RuCl_3$ and then was chemically reduced. (d) HRTEM image simulation. (e) Schematic structure model.*

However, inner diameters of MWCNTs [43] are comparatively large (in general in the range 5–50 nm) and the filling of the much smaller inner diameter SWCNTs (in general in the range 1–1.5 nm) that were discovered in 1993 [44,45] therefore appeared more challenging. It actually took five years following the reporting of filled MWCNTs for the first two definitive examples of filled SWCNTs to be reported (Figure 5a.2). One was the incidental discovery of the ability of fullerenes to diffuse and pack into SWCNTs, thereby forming the so-called 'peapods' [46]. The other, involving the hydrogen reduction of $RuCl_3$ introduced into pre-opened SWCNTs from solution was reported in the same year [10].

By analogy with the accepted notation for endofullerenes, SWCNTs filled with fullerenes were symbolized as C_{60}@SWCNTs [47], which rapidly became the overall notation for any kind of X@CNT, where X is the chemical symbol of the filling material (or, sometimes, an accepted abbreviation for a chemical compound) and CNT is the nanotube type, as described previously.

5a.2.2 The Expectations with Filling CNTs

In a similar fashion to the preparation of decorated nanotubes, in which the latter are essentially considered as a substrate, nanotubes can be considered with respect to their inner cavity, that is, an empty volume that can be used as a template or 'nanomould', and/or as a 'nanoreactor' (i.e. for the chemical transformation of an inserted material) for the synthesis of nanomaterials. Due to the immense length/cross-section aspect ratio of nanotubes, inserted materials are forced to adopt a nearly one-dimensional morphology, especially when considering SWCNTs whose internal cavities are consistently smaller than those of MWCNTs and whose aspect ratios are considerably longer. The host nanotubes may also act as nanocapsules protecting the contained materials from any reaction with the surrounding medium, typically (though not exclusively) oxidation by

contact with the atmosphere, as well as dissolution of the filling material in aqueous or nonaqueous solvents. Nanotubes may therefore make possible the synthesis of nanowire-like materials that could never exist if not encapsulated. Indeed, metallic nanowires of 1 nm in diameter would rapidly turn into oxide nanowires or would even possibly collapse, as recently demonstrated by attempts to remove the carbon sheath from filled SWCNTs [48]. In both cases, chances are high that any peculiar property is lost. Generally speaking, growing phases within a very confined volume allows for the formation of new nanomaterials to be expected because of the possibility opened to enforce and stabilize new combinations of chemical elements, to enforce and stabilize novel crystal structures for regular chemical phases and to deform and stress lattices within regular structures.

Of course, new nanomaterials are mainly valuable if they come with new, altered or enhanced physical properties. The latter are expected from the stabilization of otherwise impossible new chemical compositions, structures, or morphologies. Typical examples are (i) the ballistic transport behaviour from the one-dimensional structure, which prevents electron scattering; (ii) the very unusual surface-atom to core-atom ratios, which may even reach an infinite value, (e.g. all the atoms of the structure can effectively be 'surface atoms'), and (iii) the protection by the carbon sheath from the surface adsorption of disturbing molecules. Typical anticipated and realized benefits regard nanowires made from magnetic elements or compounds and charge-transfer electronic interactions with the encapsulating graphene lattice and the guest materials.

Finally, should encapsulated phases not exhibit new structures, chemical composition or physical properties, encapsulation may provide external reactants peculiar access conditions to the filling materials, thereby controlling the behaviour of the latter by controlling the interaction kinetics with the surrounding medium. Of course, this could occur in a negative manner, for instance, regarding the filling material chemical reactivity that may be more or less inhibited in spite of the nanosize because of the presence of the carbon sheath. On the other hand, this modified behaviour regarding chemical reactivity may be useful to some applications, for instance, slowing down diffusion kinetics and/or chemical reactivity may be very valuable in fields such as chemical catalysis, drug or pesticide delivery, and so on.

Hence, encapsulating materials in CNTs is likely to promote new phases, new structures, new properties, and/or new behaviours. However, any of these features will be more likely as the tube cavity diameter is smaller. Filling nanotubes whose inner cavity is below ~2 nm wide, as is encountered in most of SWCNTs and DWCNTs, will therefore be preferably considered below. Detailed review papers specifically dealing with filling MWCNTs may be found in the early literature [49,50].

5a.2.3 Filling Parameters, Routes and Mechanisms

5a.2.3.1 Filling Strategy

Various ways of filling nanotubes may be considered, depending on the physical properties of the material being inserted, the cavity diameter to be filled, the cost issues (if for commercial purposes) and the capabilities of the methods themselves, with all parameters being more or less interdependent.

Materials can be inserted into CNT cavities as a solid, liquid, or vapour. Hence, relevant physical properties of the materials filling the nanotubes are primarily solubility, melting

point, boiling point and of course, decomposition temperature, which should not be reached. When liquids are involved (i.e. as either a molten or dissolved material), a subsequent property of the utmost importance to consider is surface tension. It was experimentally observed that the surface tension (γ) of liquids should be below 100–200 mN m^{-1} in order to wet MWCNTs [40] while supporting the idea that the capillarity-driven mechanisms for filling nanotubes with liquids are obeying the Young-Laplace law and equations. Later on, this surface tension threshold was more precisely defined as 130–170 mN m^{-1} for SWCNTs [39]. In addition to surface tension, the viscosity of the liquid material is also interesting to consider as a parameter presumably important in the filling event, at least regarding the filling kinetics. In addition, it might also be interesting to know the vapour pressure of the material to be inserted to estimate, if needed, whether some vapour was introduced along with the liquid. These aspects will be discussed further in the following sections.

The nanotube inner diameter is obviously an important parameter because, in the first instance, it will determine the ultimate diameter of the basic entities (such as molecules, as a vapour or in solution, or the cross-sectional diameter of any included crystals) able to enter the nanotube cavity. On the other hand, it is also quite important when filling with liquids because it will contribute to the determination of the respective filling efficiency. Previous studies have actually proposed that a minimum inner diameter for the nanotube to fill is required [38]. Because this cut off value depends on the surface tension of the liquid involved, it does not correspond to a single value, hence, no 'magic' number for the nanotube diameter can be provided. For instance, threshold nanotube inner diameters were calculated to be 0.7 and 4 nm for molten V_2O_5 ($\gamma = 80$ mN m^{-1}) and molten $AgNO_3$, respectively [38,50].

In addition to the intrinsic cost of the starting materials, product recyclability and energy supply for thermal steps, an important feature for cost issues is the number of steps included in the filling process. The latter aspects may drive the selection of the filling process but may also drive the nanotube synthesis process because some may allow in situ filling, that is, these are able to fill nanotubes while they form.

5a.2.3.2 In Situ Filling Processes

Filling nanotubes in situ is interesting because it is a single-step synthesis procedure; it leaves the nanotube sheath intact and, depending on the synthesis process, closed (for arc-prepared nanotubes) or opened at one end only (CCVD-prepared nanotubes), thereby protecting as far as possible the encapsulated material from any contact with the surrounding post-synthesis atmosphere and it allows nanotubes to be filled with elements whose surface tension is high enough to prevent filling by wetting methods (see next).

In situ filling was one of the two early ways that foreign materials were introduced into MWCNT-type nanotubes simultaneously with their synthesis. Two techniques permit this: one is the electric arc process [51] and the other is the CCVD process (Figure 5a.3) [52,53]. The latter is rather limited because it most often corresponds to specific conditions for which the excess metal catalyst that is needed to grow the nanotubes is trapped and encapsulated inside them. Therefore, filling nanotubes this way is basically restricted to materials that are catalysts for carbon formation, typically transition metals such as Ni, Co, and Fe, although examples of other types of materials encapsulated this way can be found in the literature (e.g. Cu and Ge in [53]). Because catalyst metals for carbon are mainly ferromagnetic materials, it is actually quite a convenient way to produce ferromagnetic nanowires encapsulated in nanotubes [52,54,55] otherwise difficult to obtain (see next).

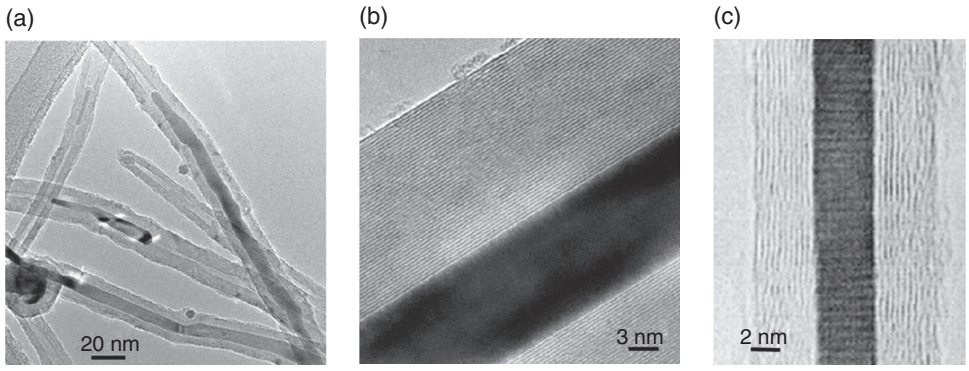

Figure 5a.3 *(a) Low-magnification TEM image of in situ filled MWCNTs obtained via a CCVD-related process. The filling material is pure α-Fe (bcc Fe crystals). (b) High resolution of one of the Fe@MWCNTs in (a). The perfection of graphenes from the surrounding carbon nanotube is shown. Lattice fringes of the contained iron crystal are not seen because of the high Z number of Fe that makes it barely transparent to electrons. The material was prepared by P. Watts (University of Sussex) following the procedure reported in [52]. (c) High resolution TEM image of an in situ filled MWCNT obtained via an electric arc plasma process. The filling material is a single crystal of pure chromium [57]. Modified with permission from [13] Copyright (2006) Cambridge University Press.*

The electric arc plasma process consists in drilling a coaxial hole within the graphite anode and filling it with the ground, desired element (or a mixture of it with graphite powder). Once the electric arc is run using conditions (current, voltage, pressure, and atmosphere) similar to that used to produce fullerenes, the MWCNTs that usually grow as a cathode deposit are found partially filled with the desired element. However, the efficiency and control of the filling process is lower than for the CCVD-related method, probably because of the huge temperature gradients that are typical of the plasma zone in arc-related processes, and that are also responsible for the heterogeneity in the diameter distribution of the MWCNTs synthesized that way. A specific requirement for achieving successful in situ filling in arc plasma processes is that some sulfur is present, added or naturally contained as an impurity (e.g. originating from the pitch used as a binder) within the graphite anode, otherwise the filling mechanism may fail [56,57]. As opposed to the CCVD-based method, the electric arc method is hardly able to form hybrid MWCNTs encapsulating transition metals such as Fe, Ni, or Co, although some rare exceptions may be found (e.g. with Co [51]). The reason is that as soon as such a metal is introduced into the system (i.e. by doping the graphite anode with it), it forms C-metal solid solution droplets that are encapsulated as carbides within the MWCNTs growing at the cathode, or that escape the plasma zone to subsequently promote the growth of (empty) SWCNTs from them. That is actually how SWCNTs were incidentally discovered, that is, as by-products of attempts to fill MWCNTs with transition metals (i.e. Fe [44] and Co [45]).

The CCVD method and the electric arc method conveniently complement each other because the former is mainly able to produce transition metal-filled MWCNTs, whereas the latter is not but is mainly able to produce MWCNTs filled with many other elements [51–57]. On the other hand, both methods exhibit severe limitations. One is that only single elements

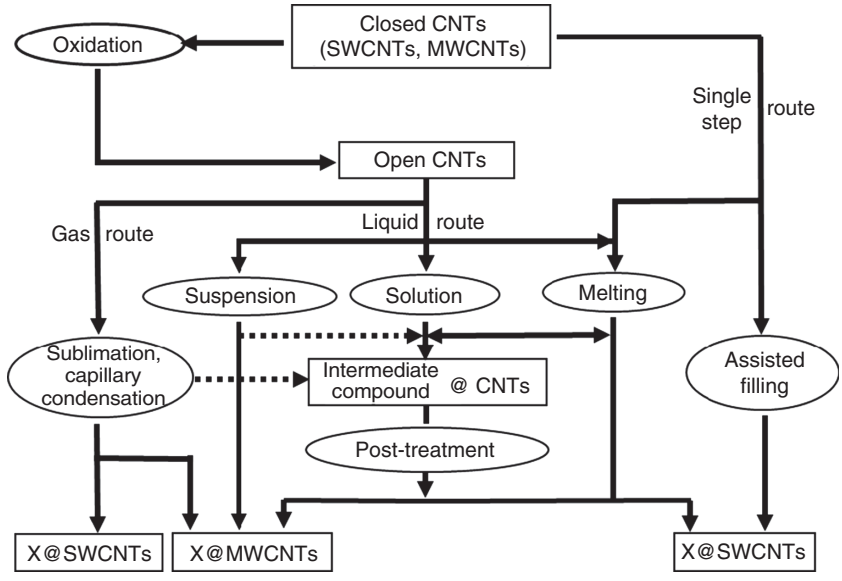

Figure 5a.4 *Sketch of the various experimental routes that are possible for the ex situ filling of carbon nanotubes. The rectangles indicate obtained materials while ovals indicate treatment steps. Modified with permission from [13] Copyright (2006) Cambridge University Press.*

or carbides, as stated above, are able to be inserted because of the requirement of being a carbon catalyst for the CCVD process or because of the high temperatures involved (for the electric arc plasma process) that do not allow oxides or salts to form. Typically, inserting multi-element compounds is not possible, nor is inserting labile materials. Another major limitation is that synthesizing filled SWCNTs this way is nearly not possible and when it is, it comes with very low yield, in the range of a few percent of the obtained product. Examples in the literature are very scarce and involve the electric arc process only. One involves the spontaneous formation of peapods obtained during arc experiments designed to grow SWCNTs [58,59] and the other is the encapsulation of Bi in SWCNTs grown with Co as catalyst [11], both Co and Bi having previously been introduced into the graphite anode, as described here.

The severe limitations related to in situ filling, specifically regarding SWCNTs, have therefore promoted the development of ex situ filling processes, as we shall see in the next section.

5a.2.3.3 Ex Situ Filling Processes

Ex situ filling is the most versatile route because it makes possible the ability to insert nearly any kind of material into nearly any kind of nanotube. This basic principle was acknowledged long ago when the first fillings of MWCNTs were achieved [20,49–51]. Figure 5a.4 summarizes the various ex situ filling pathways that will be described in the subsequent sections. Ex situ filling can be carried out following one-, two-, or three-step procedures, not mentioning a final cleaning step, which is needed for any of the ex situ methods to remove any extraneous material, by means of washing or dynamic vacuum

heating (the latter may be preferred for avoiding a liquid phase step that often comes with residuals, and the filtration step that compacts the filled SWCNT material obtained).

5a.2.3.3.1 Previous Opening of the Tubes Except for single-step filling procedures, and unless starting nanotubes are naturally opened because of the specificity of the nanotube synthesis process (e.g. templating), the first step for ex situ filling of nanotubes is dedicated to the prior opening of the latter, which can be achieved in two main ways, documented since the early days of filling MWCNTs [16,19,60]. These consist of (i) thermal treatments in an oxidizing gas phase (air or O_2) [41] or (ii) reaction with liquid reactants that are oxidizing for polyaromatic carbon materials, typically, acids such as concentrated nitric (preferred) or sulfuric acid [60] or a mixture of both. The latter can also include oxidants such as hydrogen peroxide, potassium permanganate, fluoric acid/bromine fluoride mixture, osmium tetroxide, and so on [61]. Gas or liquid phase oxidation procedures are efficient in opening MWCNTs or SWCNTs, although conditions have to be more severe for the former because of the higher number of graphene walls to penetrate. However, liquid phase oxidation tends to generate residuals that may more or less coat the nanotubes, thereby hindering subsequent treatments (including filling) or investigations (such as TEM). In this respect, gas phase oxidation is generally preferable and is the dominant technique for opening SWCNTs. For instance, subjecting raw SWCNTs obtained from arc process to a 380°C thermal treatment (including 1 h of isothermal) in air within an open tubular furnace allowing natural convection was proven in our laboratory to be able to create openings as wide as 0.7 nm or more in SWCNTs from the arc method with an overall weight loss in the range of 40%. This mass loss was not only from the nanotubes and varied according to the amount and type of carbon impurities and catalysts (if any) employed. Such a treatment allows SWCNTs to be subsequently filled with fullerenes with a filling efficiency that may reach ~90–95%. Interestingly, because purification procedures that are carried out on SWCNTs to remove carbon by-products (and catalyst remnants) are oxidizing treatments as well, purified SWCNTs available from commercial suppliers (e.g. Nanocarblab in Russia) may exhibit openings that are sufficient to allow them to be filled with high efficiency without needing any further treatment but the filling step.

Considering the comparatively high inertness of the graphene lattice toward chemical oxidation, opening occurs at the location of structural defects (typically five- or seven-membered rings) whatever the tube type. Pentagons are obviously found at the tips of nanotubes as a requirement to curve and close the graphenes involved, making nanotubes naturally able to be opened from the tips. However, a major difference regarding the behaviour of MWCNTs versus SWCNTs upon oxidation is that the former are able to open from the tips only, whereas SWCNTs are able to open from the tips and the side walls. Indeed, as discussed earlier [62], several experimental results such as TEM investigation, behaviour under electron irradiation, and titration of acid-treated SWCNTs have shown the presence of side defects to be very likely (typically, heptagon-pentagon ring pairs or double pairs, the latter corresponding to the so-called Dienes defects), with an average proportion of one chemically attackable site every 5 nm along a given SWCNT wall. Filling of SWCNTs by this route was further supported by calculations and modelling [63]. In contrast, even should every graphene tubule making up the composite wall of a MWCNT be defective, the chance for the defects from each graphene to superimpose at a given location of the wall to create a site for side opening is nil, except in the MWCNT

tip region where pentagons obviously superimpose from reasons related to geometric constraints at the sites of the nanotube closure.

5a.2.3.3.2 Filling by Means of Gas Phase Processes Filling nanotubes via the gaseous phase consists in putting in contact the previously opened nanotubes (i.e. MWCNTs, DWCNTs or SWCNTs) and the vapour of the material to insert in them, for instance, in a Pyrex or quartz vessel that should be evacuated (primary or, preferably, secondary vacuum) before being sealed, and then heated up to the desired temperature which will typically be either the vaporization or sublimation temperature of the filling material, or slightly above. This is the way peapods (e.g. C_{60}@SWCNT) are usually prepared [64]. For a filling material such as fullerenes, which exhibit high electronic affinity with the graphene lattice (i.e. the nanotube surface) insertion into the SWCNT cavity was proven to be a surface diffusion-driven mechanism [64]. Hence, it is highly dependent on temperature and time, but weakly dependent on the partial pressure of filling material vapour. Therefore, operating at a not-too-high temperature is necessary to minimize temperature-induced stochastic movements of the filling molecules and to give them a sufficient residence time on the nanotube surface to enable them to find the entry ports. A long processing time, in the range of several hours to two days, is therefore necessary to achieve high filling rates (sometimes close to 100%) provided a sufficient amount of filling material is supplied. For other types of materials to insert that do not exhibit the same affinity for the graphene lattice (e.g. $ZrCl_4$ [65], Se [66], or Re_xO_y [67]), the filling mechanism is therefore slightly different and relates to capillary condensation. In the latter, a high partial pressure of the material to be inserted has to be developed at the vaporization/sublimation temperature or above, and the vapour condenses into the capillary porosity (i.e. the tube inner cavity) when the system is cooled down. High filling efficiencies, along with shorter processing times (e.g. with respect to peapod synthesis), are therefore expected for materials exhibiting high vapour pressure (e.g. Se [66]). Examples of quantitative filling are provided in Figure 5a.5.

The gas phase route has many advantages: its relative simplicity (basically two steps, i.e. opening and filling), its potentiality for a high filling rate and high purity/homogeneity of the filling material, and also the absence of the requirement that the material meet the threshold surface tension requirement (see the next section). It is applicable to SWCNTs and MWCNTs, although examples for the latter in literature are scarce [66,68,69]. Conversely, a major drawback of the method is the need for the filling material to exhibit vaporization or sublimation temperature below ca. 1000°C–1200°C, to minimize the chances for healing the nanotube openings and/or for possible reactions with carbon. Inserting compounds this way is limited as well because candidate materials such as oxides are often high temperature refractories or, on the contrary, compounds such as salts are barely able to vaporize or sublime without decomposing.

5a.2.3.3.3 Filling by Means of Liquid Phase Processes The major characteristic of the liquid phase methods is their close dependence on the physical interaction between the filling liquid and the encapsulating solid, typically via the Young-Laplace law for capillary wetting. As soon as a solvent is involved, as for the suspension and the solution methods (see next), wetting is not supposed to be a problem because surface tensions of the usual solvents are below 80 mN m^{-1}. However, viscosity is certainly another parameter assumed to play a leading role, yet it has been scarcely considered in the literature dealing with the topic.

The *suspension method* is dedicated to filling nanotubes with nanoparticles. Although examples (thus far involving MWCNTs only) are still limited because quite recent [70,71],

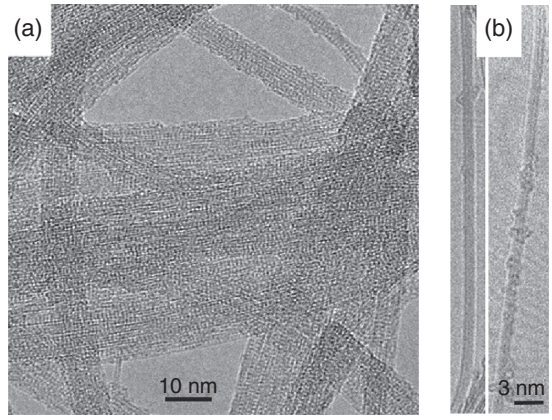

Figure 5a.5 *Examples of hybrid SWCNTs with high filling rates obtained via the gas phase route. (a) Low magnification of C_{60}@SWCNT (peapods) material prepared by the sublimation method (450°C, 24 h). The periodically dashed contrast of the bundles is due to the overall presence of the fullerene molecules aligned within the SWCNT inner volume. High resolution images of such peapods are given in Chapter 5b (image credit: M. Berd, CEMES-CNRS). (b) Low resolution, high magnification images showing two examples of a full filling over lengths longer than 60 nm with a sample of Se@SWCNTs prepared by capillary condensation (800°C, several hours). Modified with permission from [13] Copyright (2006) Cambridge University Press.*

filling rates can be fairly high. This is not very surprising considering the large diameters of the MWCNTs being filled in comparison to the small particle size of the introduced material (Figure 5a.6). In related experiments, open nanotubes were put into contact with a suspension of nanoparticles in a liquid at room temperature, the latter being evaporated during the experiment and/or afterward. Low volume concentrations of particles in the suspending fluid were used to maintain a low viscosity. The high filling efficiency is attributed to the combination of capillary forces [71] possibly added with the effect of the concomitant fluid evaporation [70], the latter being assumed to drive a continuous flow of fresh suspension from the outside to the inside of the tube.

The method is interesting because it is quite simple (two steps, opening and filling) and efficient but it comes with severe limitations related to geometrical constrains and the morphology of the filling material feedstock. Indeed, nanotubes to be filled will be limited to MWCNTs, unless clusters less than 1 nm large in diameter can be produced to fill pre-opened SWCNTs. One related example has actually been reported already in which nanohorns (nanohorns are short, tapering single-wall nanocapsules [72]) were partially filled with 1 nm or less Gd-containing clusters [73]. On a more positive note, obtaining encapsulated nanowires using this approach will be possible once nanoparticles will be inserted and aligned within CNTs whose inner diameter matches that of the nanoparticles, while the chemical nature of the nanoparticles would allow them to melt and coalesce upon annealing at a temperature range that does not damage the CNTs. Generally speaking, the trickiest part of the procedure is the need to be able to prepare nanoparticles of the desired materials before the filling step. This is not common knowledge yet. However, some are now commercially available (e.g. Sigma-Aldrich), even

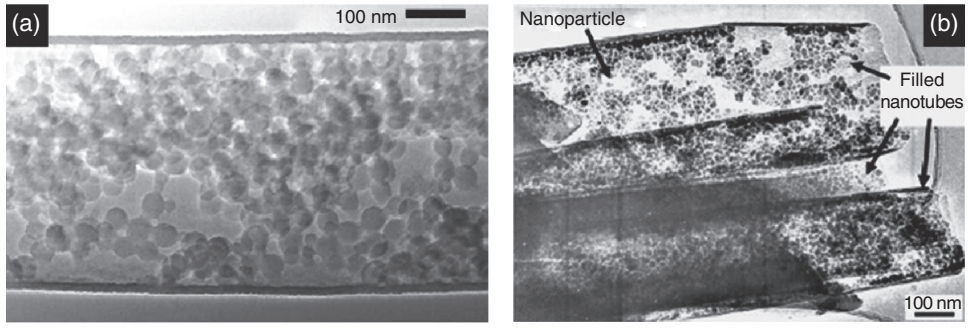

Figure 5a.6 *Examples of MWCNTs filled with nanoparticles via the suspension method (liquid route), taken from pioneering works. (a) Polystyrene nanobeads initially suspended in ethylene glycol (reprinted with permission from [53] Copyright (1996) Elsevier Ltd). (b) Fe_3O_4 nanoparticles initially suspended in water- or organic-based solvents, the whole making so-called' 'ferrofluids' (reprinted with permission from [54] Copyright (1998) The Royal Society of Chemistry).*

as a ready-to-use suspension (e.g. so-called ferrofluids, as supplied by Ferrotec Corporation, Japan, for instance). At any rate, this field is just starting, and interesting developments are anticipated. Smaller diameter MWCNTs or large-diameter SWCNTs should be able to be used, annealing post-treatments should possibly be able to transform the packed nanoparticles into single nanorods in MWCNTs with narrow inner cavity, and so on.

The *solution method* is quite similar to the latter and consists of putting into contact a concentrated solution of the desired materials with the previously opened nanotubes. This generally requires considering soluble derivatives of the materials ultimately wanted to fill the nanotubes (MWCNT or SWCNT), such as salts (halides or nitrates, usually). It is the compulsory method to use when the desired filling material does not present the appropriate physical constants for inserting itself via the gas phase route (see Section 5a.2.3.3.2) or the molten phase method (see next), both of which should be preferred for their higher filling efficiency and fewer number of steps. Examples where the desired filling material is directly inserted into nanotubes via the solution method are actually seldom, and post-treatments (most often calcination as in [74] or reduction as in [10,11,75] but also other treatments such as photolysis or electron irradiation, as in [65,67]) are most often necessary to obtain the hybrid nanotube with the desired chemical composition (Figures 5a.7(a) and 5a.7(b)). This method was actually the very first one used to deliberately fill SWNTs with Ru from $RuCl_3$ [10] and has been widely used since then.

An interesting feature of the solution method is that it is can be operated at either room or colder temperatures. This allows nanotubes to be filled with thermally unstable materials (e.g. fullerenes grafted with organic functionalities [76,77] or $N@C_{60}$ endofullerenes [78]). A valuable alternative is to keep operating at mild temperature conditions (50°C) but use high pressure (150 bars) to be able to replace regular solvents (water, acids, chloroform, toluene, etc.) with supercritical CO_2 [79,80]. The latter is a very powerful solvent and exhibits a high penetrability in nanopores thanks to its very low viscosity and low surface tension. Although operating times as long as several days might be necessary [79], the method is to be considered as being applicable to a large range of compounds.

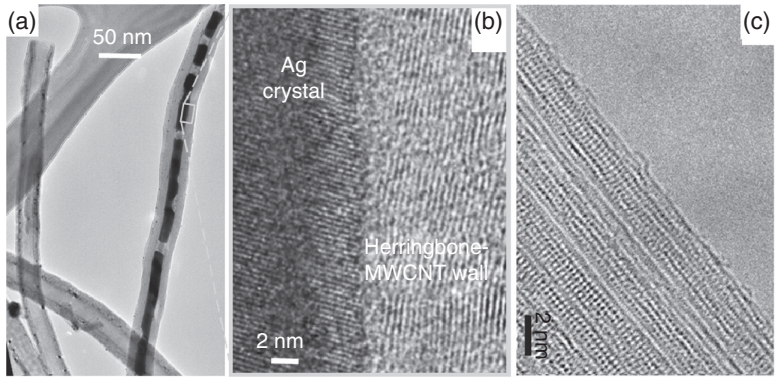

Figure 5a.7 *(a) Example of CCVD MWCNTs partially filled with Ag via the solution method (liquid route): nanotubes were soaked in a water solution of silver nitrate upon stirring for 48 h at room temperature and then calcined at 300°C in vacuum. (b) High resolution detailed portion of the nanotube filled in (a), showing that each of the encapsulated Ag rods seen in (a) are monocrystals (reprinted with permission from [13] Copyright (2006) Cambridge University Press). Electric arc SWCNTs were also able to be filled using the same procedure [13]. (c) High resolution TEM image illustrating the high filling rate obtained for KI@SWCNT using the molten phase route combined with thermal cycling, by showing a bundle of SWCNTs, most of them being highly filled with elongated KI single crystals.*

Finally, although the solution method is intrinsically multi-stepped to generally account for opening, filling and post-treating the nanotubes, it could also be made into a single step in some specific cases which allow raw nanotubes to be opened and then filled during the same process. For instance, when considering filling in solution, this requires the solution to be able to contain the dissolved filling material as well as to be oxidizing toward the nanotubes. This was achieved in [18] by soaking raw SWCNTs from arc within a super-saturated solution of CrO_3 in concentrated HCl. Both reacted to form CrO_2Cl_2, which is known for being highly oxidizing for polyaromatic carbon, including graphite [81], hence resulting in opening the SWCNTs. The excess CrO_3 was then able to enter the SWCNT cavity, thereby forming CrO_x@SWCNT hybrid nanotubes.

To summarize, the solution method is quite useful as an alternative when other routes (i.e. the gas phase route described in Section 5a.2.3.3.2 and the molten phase method described below) are not possible because of the inappropriate physical properties of the desired filling materials. Thanks to the large variety of compounds that can be found soluble in some solvent, the method appears widely applicable. Except for very specific cases, the method has to be multi-stepped (three steps), which can be a drawback. Nevertheless, the main limitation lies in the concomitant filling with the solvent molecules (along with the dissolved desired material), which cannot be avoided. As a common observation [64,66], this prevents high filling rates from being achieved.

As opposed to the solution method, the *molten phase method* allows high filling rates to be achieved, was among the first methods used to fill MWCNTs (with PbO [19]) and was subsequently demonstrated to be highly successful even for SWCNTs (Figure 5a.7(c) and Figure 5a.8). For instance, SWCNT filling rates as high as 70% were reported for KI [82]

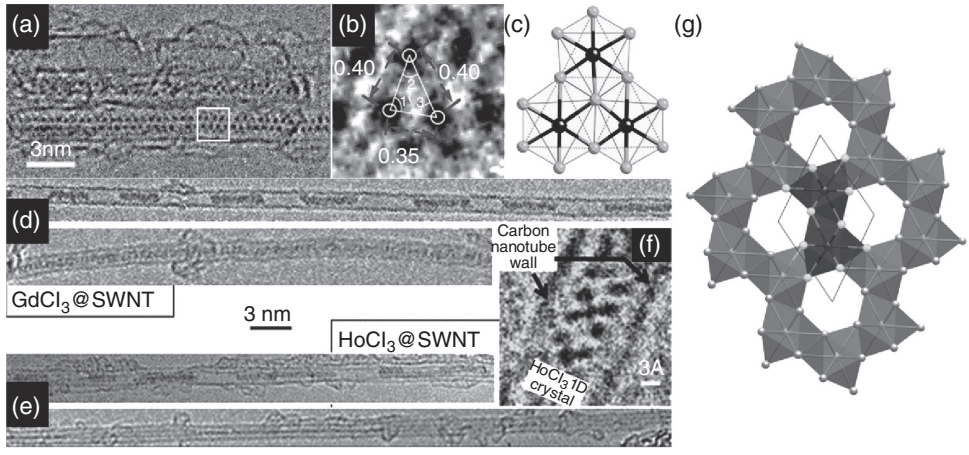

Figure 5a.8 *Examples of SWCNTs filled with lanthanide chlorides via the molten phase route: nanotubes were sealed under vacuum in a quartz ampoule along with the ground material to fill them with, and were then heat treated for 24 h. (a), (b) and (c) HRTEM image, detail and corresponding structure model of $TbCl_3$@SWCNT obtained at 588°C. (d) $GdCl_3$@SWCNTs obtained at 700°C. (e) and (f) HRTEM images of $HoCl_3$@SWCNTs obtained at 820°C. Filling materials can form continuous nanowires (bottom region in (a) and bottom images in (d) and (e)) or short segments somewhat periodically displayed (top image in (d) and (e)). The crystal structure of these materials is very interesting and often corresponds to reduced fragments 'selected' from the bulk crystal structure, as shown in by the selection in (f). Likewise, the $TbCl_3$ fragment derived in (c) is a reduced coordination version of a fragment derived from the regular $P6_3/m$ bulk structure shown in (g). Images (d) to (f) are reprinted with permission from [13] Copyright (2006) Cambridge University Press.*

although cumulating filling cycles were necessary to achieve it. This makes the method almost as efficient as the gas phase route obviously because, for both methods, only the desired filling material is entering the nanotube cavity.

The procedure is similar to that for the solution method of the gas phase route, that is putting together the previously opened (or not, see next paragraph) nanotubes and the material to fill the latter within a quartz vessel sealed under vacuum, and then heating up the whole. The temperature has of course to be above (~30–100°C higher) the melting temperature of the filling material and maintained for long times, in the range of 1–3 days (see [82–84], among others) although this may be shorter for some low viscosity materials. Such long times are necessary to account for the high viscosity that the molten materials may exhibit and that slows down the filling kinetics (specifically within SWCNTs), and also to account for cycling (Figure 5a.7(c)). Cycling does not require repeating the whole procedure and, provided a sufficient amount of the material to fill is supplied as a feedstock in the starting sealed ampoule, repeatedly operating within a limited temperature range (e.g. ± 30°C) bracketing the filling material melting temperature was shown to be enough [82]. Again, when high-melting-temperature materials, for example, metals, lanthanides, and so on, are the ultimate filling materials envisaged, compounds such as salts are the preferred materials for the filling steps because they usually exhibit lower melting points (see Table 5a.1). Hence,

Table 5a.1 *Surface tensions (and temperatures for state changes) of some elements and compounds (mostly halides and oxides) that have been investigated in the literature dealing with filling or wetting carbon nanotubes with molten materials (references to the respective data for a filling material are included within this section) (modified from [13]).*

Material	Surface tension (mN/m)	Melting temperature (°C)	Filling temperature (°C)
AgCl	113–173	560	660–560
AgBr	151	432	532–590
AgI	171	455	555
Al	860	660	
BaI_2	130	740	840
Bi_2O_3	200	825	
CaI_2	83	784	884
Cs	67	29	
CsI	69	627	727
Ga	710	30	
$GdCl_3$	92	609	659
Hg	490	–38	
K	117	336	
KCl	93	771	870
KI	70	681	781
$LaCl_3$	109	860	910
LiI	94	449	549
NaI	81	661	761
$NdCl_3$	102	784	834
Pb	470	327	
PbO	132	886	
Rb	77	39	
RbI	70	647	747
S	61	112	
Se	97	217	
Te	190	450	
UCl_4	27	590	690
V_2O_5	80	690	
$ZrCl_4$	1.3	437	487
HF	117		
HNO_3	43		

post-treatments for reducing the intermediate compounds into the desired filling materials are needed. However, interesting observations regarding the behaviour of one-dimensional crystals were already possible on such intermediate hybrid materials (see next).

A valuable alternative proposed by the Oxford Group as early as in 1999 [85] and which has been applied thoroughly since then in most of their filling experiments is to use the chemical activity of the halides toward polyaromatic carbons to get the nanotubes opened within the filling step, thereby making needless a preliminary, separate nanotube-opening step. However, this is mainly valid for SWCNTs only (and DWCNTs), for the reasons related to the number of walls already discussed above. Interestingly Grigorian et al. [86], in their early attempt to dope SWCNT bundles with iodine using the molten phase method, did not realize that this procedure could open SWCNTs. Had they demonstrated in their first paper that iodine was actually partly filling the SWCNT cavities as they showed

later [8] this work would have been cited among the pioneering studies on filling SWCNTs with foreign materials.

To summarize, the molten phase method is the second method to be preferred for filling nanotubes because of the possibilities for high filling rates, simplicity (1–3 steps, depending on the goal and the material to fill), and versatility. Its main limitation is its requirement for selecting the materials to fill (or their compounds) among those exhibiting the convenient surface tension (i.e. < 130–170 mN m^{-1} [40]) when molten at the filling temperature.

Finally, the *assisted filling methods* are worth considering because they correspond to attempts to develop original and/or simpler and/or more efficient ways to synthesize filled nanotubes. Two examples will be reported here. One by Mittal et al. [88,89] who proposed to use solutions of halides ($FeCl_3$, $MoCl_5$, and I) in chloroform subsequently irradiated with UV at room temperature. Chlorine moieties are thereby created that are able to attack the SWCNTs, allowing the filling to proceed from the dissolved material. Filling rates were actually low but the procedure was not optimized and might have included cycling, for instance. The method should be applicable to, but also limited to, any compound soluble in chloroform or other UV-sensitive appropriate solvent. The method is dedicated to filling SWCNTs (and possibly DWCNTs) only, for the same reasons as developed above for the opening by molten halides. The other example was proposed by a Japanese consortium and consists of using collisions of accelerated atoms or molecules from a plasma generated between a grounded electrode and a stainless steel plate on which SWCNTs were previously deposited. Nanotubes were filled with fullerenes [90,91] and Cs [91] this way. Oxidized and therefore opened SWCNTs were used for purity purposes only, and the method should work with raw (i.e. closed) SWCNTs as well. The kinetic energies involved are in the range of ~150 eV (for alkali metals) and filling rates can be fairly high (~50% for C_{60}@SWCNTs) with respect to the short duration of the run (~1 h). However, damaging to the nanotubes by the energetic bombardment was suspected, yet the extent of this damage was not estimated. This method is likely to be dedicated to filling SWCNTs only, considering the tremendous energy that would be needed to enter a nanotube through a multi-graphene wall.

5a.2.4 Materials for Filling

Virtually every type of material (i.e. atoms, molecules, and phases) has now been inserted into SWNT cavities. This section will provide a thorough listing of various filled nanotubes whose preparation was reported in the literature but references dealing with virtual fillings via modelling will not be provided here and whether the filling claimed in the papers cited was actual will not be discussed either. Indeed, direct evidences for filling, such as TEM imaging, were not always provided in the related papers and the successful syntheses of filled nanotubes were sometimes reported on the mere basis of spectroscopic investigations, which may be mistaken. Because the literature has become particularly abundant, citing all of the related papers was impossible and citing selected references (for example, the pioneering papers) is preferred here.

5a.2.4.1 Atoms (Isolated, or as Chains)

Encapsulating atoms so that they remain isolated is difficult because of their relative instability and demonstrating the presence of isolated atoms in SWCNTs is experimentally challenging. When not forming elongated crystals as nanowires (see next), encapsulated

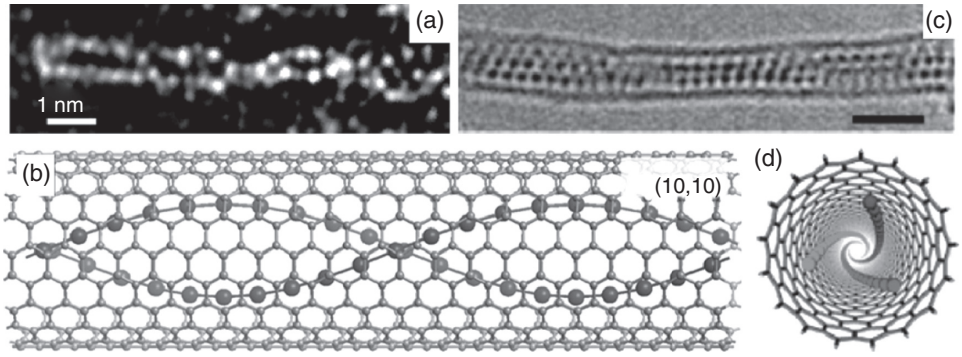

Figure 5a.9 *(a) The first example of SWCNTs filled with a double-helix chain of iodine atoms (I@SWCNT), as evidenced by means of high-resolution Z contrast TEM. (b) Side view of a model for the image in (a) considering a (10,10) tube as the containing SWCNT. (c) High- resolution TEM image of a I@SWCNT, identified as a triple-helix chain of iodine atoms. The bar is ~1.5 nm. (d) Top view of a model for the image in (c). Reprinted with permission from [87] Copyright (2000) American Physical Society (a and b) and from [9] Copyright (2007) American Chemical Society (c and d).*

atoms tend to gather as single atom wide chains, although examples of this are scarce. The first example was iodine [87], which was demonstrated to be able to adopt a beautiful helical chain structure, either single, or as double (Figure 5a.9) or even triple [9] assemblies within the same tube, presumably from commensurability situations between the I-I distance in the chain and some peculiar periodicities of the graphene lattice [87]. Based on this pioneering work, a similar structure was assumed for encapsulated Cs chains prepared later [91]. However, the formation of chains may be prevented and Cs atoms may remain as isolated, observable atoms if the latter are encapsulated along with large and low-reactivity molecules such as fullerenes, which sterically obstruct the filling pathway and do not favour the bonding or adsorption of the Cs atoms to their surface [92]. Isolated K atoms were observed similarly, that is, in SWCNTs concomitantly filled with both fullerenes and potassium [93,94].

5a.2.4.2 Molecules (Isolated, or as Chains)

Except for some rare examples whose motivation was more related to typology issues (e.g. filling BN- or C-MWCNTs with fullerenes [68,69]), filling nanotubes with molecules was and still does principally involve SWCNTs. For most of the following filling materials, the goal was generally to introduce electron donor or acceptor molecules, and thereby to tentatively modify the electronic structure of the subsequent hybrid nanotubes to obtain peculiar electronic behaviours via band gap modulations and charge transfers. The first molecules ever inserted into SWCNTs were C_{60} fullerenes [46,64] thereby forming the so-called nanopeapods [Figures 5a.2(a), and Chapter 5b]. Many fullerene-related filling materials have then followed, including higher fullerenes until C_{90} [95], endohedral fullerenes such as $N@C_{60}$ [78], $Sc_3N@C_{80}$ and $Er_xSc_{3-x}N@C_{80}$ [96], $Dy_3N@C_{80}$ [97], $Gd@C_{82}$ [95,98], $La@C_{82}$ and $La_2@C_{82}$ [99], $Dy@C_{82}$ [95,100], $Sm@C_{82}$ [101,102], $Sc_2@C_{84}$ [102], and $Gd_2@C_{92}$ [103,104], functionalized fullerenes such as [cyclopropa-C_{60}-dicarboxylic

acid diethyl ester (abbreviated as $C_{61}(COOEt)_2$@SWCNT [79]) and fullerenes grafted with a retinal chromophore [77].

Regarding the former category (i.e. higher fullerenes), C_{90} is the largest (empty) fullerene deliberately inserted in SWCNTs so far [95], while Gd@C_{92} endofullerenes were the largest such species encapsulated in this category [103,104]. Elongated capsules obtained from the in situ coalescence of encapsulated C_{60} upon various processes (see Chapter 5b) may also be considered higher fullerenes (for example, consider the formation of C_{120} from the coalescence of two C_{60} molecules). In this regard, the ultimate higher fullerene possibly encapsulated is an inner capped SWCNT, thereby making the whole become a DWCNT (that could also be abbreviated as SWCNT@SWCNT!).

Although fullerenoids are the most popular filling molecules, several other organic molecules have been recently inserted in SWCNTs, including metallocenes [4,5,12,96, 105–108], octasiloxane [6], *ortho*-carborane and related molecules [2,3], fulvalenes [109], Zn-diphenylporphyrin [1,110], Pt-porphyrin, rhodamin-6G, and chlorophyll [110], and squarylium dye [7].

In addition, some of the works deal with filling SWNTs with molecules that are gaseous at room temperature, as opposed to those listed above which exist in the solid phase. However, except for hydrogen, whose adsorption by SWCNTs, MWCNTs and carbon nanofibres was extensively investigated for reasons related to the perspective of a new era based on hydrogen economy [111], gaseous molecules investigated are still scarce, but include Xe [112], O_2, and N_2 [113], and so on. Even more critically than for any other filling material, filling SWCNTs (or MWCNTs) with gaseous molecules whose physisorption is the main interaction mechanism with the nanotubes makes highly questionable the actual location of the adsorbed molecules. Considering SWCNT bundles, the inner nanotube cavity is only one of four distinct adsorption sites identified from their various adsorption energy potential (see Figure 1.20 in Chapter 1, and [114]). In addition, the demonstration of the actual adsorption of some gaseous molecule onto or within any material, including CNT, is generally indirect, via so-called gravimetric or volumic methods, with which the only evidence for gas adsorption is obtained from the weight gain of the nanotube sample or the measured consumption of a known volume of feedstock gas, respectively. This opens wide the door for misinterpretations from various sources or errors independent from the tested material (e.g. leaks, H_2O traces, impurities, buoyancy effects, etc.), which are likely to contribute significantly (or even prevalently) to the demonstration of an adsorption phenomenon onto nanotubes. That is why the supposedly ~7 wt.% filling of gaseous H_2 in SWCNTs reported as early as 1997 [115] has to be considered with caution, first because it was later on demonstrated that the high amount of H_2 claimed for being trapped in the SWCNTs resulted from a misinterpretation [116], and also because there was no demonstration of the effective filling, that is, the insertion of H_2 molecule gas into the SWCNT inner cavity was not demonstrated, meaning that the H_2 molecule adsorption could have occurred in one of the other three adsorption sites mentioned above as well. It was demonstrated only far later that the inner cavity of the SWCNTs does contribute as an adsorption site for H_2 [117], yet the total amount of adsorbed hydrogen molecules remains low (less than 1 wt.%) at least at room temperature. The adsorption of permanent gases in nanotubes will not be considered further in this chapter.

Discrete molecular anions were also introduced and imaged within DWCNTs [118]. The type of anion observed is a Lindqvist ion which belongs to the family of inorganic poly-oxometalate (POM) ions which are effectively ordered oxide clusters built up of metal

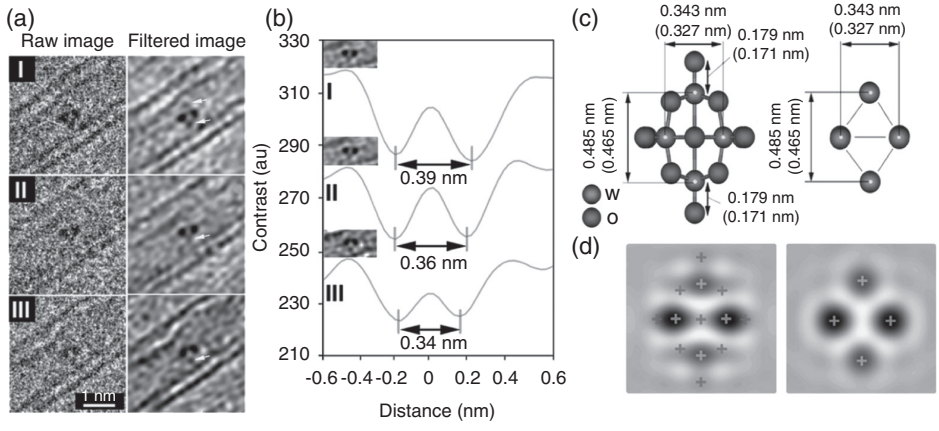

Figure 5a.10 *(a) A sequence of HRTEM images (left) obtained from a single $[W_6O_{19}]^{2-}$ anion locked into position within the capillary of a DWCNT shown with Fourier-filtered images (right). (b) Line profiles produced through equatorial spots corresponding to pairs of W atoms. (c) Structure models of the $[W_6O_{19}]^{2-}$ anion with oxygen included (left) and excluded (right). Selected bond distances are included for the unrelaxed anion (in brackets) and the relaxed anion (from MD). (d) HRTEM image simulations produced at ideal defocus from the structure models in (c) showing the effect of including oxygen in the image simulation calculation. When the oxygen atoms are included (left simulation), the centre of the spot contrast in the equatorial W atom pairs are distorted outwards towards the three terminal oxygen atoms on each side of the anion. When the oxygen atoms are not included (right simulation), there is relatively little distortion of the W positions (red crosses = O; green crosses = W). For a better understanding of the figure, please refer to the colour plate section. Reprinted with permission from [118] Copyright (2008) American Chemical Society.*

oxide polyhedra in various face, edge and corner sharing configurations. As a result of the corresponding oxidation states of the heavy metal cations and charge balancing with the surrounding O^{2-} atoms, these anions almost invariably have a net negative charge which is counterbalanced, typically, by organic counterions, for example $[NBu_4]^+$, or more complex counterions, such as dendrons. The resulting anions are nonspheroidal (cf. the fullerenes or endofullerenes) and are comparable in size to the inner diameter of the containing nanotube. As a result of this external morphology, the anions can 'lock in' to position within sterically matched nanotube capillaries and this has the advantage that the structure of the anion can be studied with greater clarity than other more mobile species not rigidly fixed in position including, for example, the metallocenes, carborane, fulvalenes, and so on, mentioned above and also many of the fullerene and endofullerene examples mentioned in this section and Chapter 5b, in particular when the included species is not sterically matched with the encapsulating nanotube (i.e. consider the inclusion-nanotube spatial relationships in Figure 5a.1(b)–(e)). In the recent example, a Lindqvist ion of the form $[W_6O_{19}]^{2-}$ (i.e. a 'super-octahedra' comprised of six WO_6 octahedra fused together at their faces) was inserted into DWCNTs and then imaged by HRTEM (Figure 5a.10). As a result of the locking-in it was possible to study the separation between two atom columns each containing just a pair of W atoms. Once the contribution of the HRTEM image contrast due to the oxygen atoms was taken into account, it was possible to verify that a small expansion had

taken place in situ, possibly associated with an electronic interaction between the nanotube and the encapsulated anion. The nature of this interaction is currently the subject of ongoing theoretical investigations.

5a.2.4.3 Pure Elements (as Nanowires or Nanoparticles)

As opposed to encapsulated iodine or caesium atoms, which were demonstrated to gather as monoatomic chains (e.g. Figure 5a.9), other elements may form wires when encapsulated in SWCNTs, most often crystallized metals (e.g. Figures 5a.2(b) and 5a.8(c)). SWCNT- (or DWCNT-) encapsulated elements include Ru [10], Bi [1311], Co [15], Se [66], Ag [74,75,85,119,120], Au [75], Pt [75], Pd [75], and Fe [12,121,122] among others. The Bi and Se fillings are distinct from the other pure element fillings because they were inserted either from the liquid phase or the vapour phase, whereas the other fillings were inserted as intermediate compounds (e.g. salts) in a first step, and then formed in situ via post-treatments (e.g. thermal treatment and/or hydrogenation). The reasons why, upon encapsulation in SWCNTs, some atoms such as Bi and Se form several atom-large nanowires while other atoms such as I and Cs form single atom chains have not been fully discussed. The reasons do not lie in discrepancies in the respective, average diameters of SWCNTs, because the latter mainly originate from the regular electric arc method that provides SWCNT diameter distributions in the 1–2 nm range with a median diameter of ca. 1.4 nm. The reasons neither lie in the respective filling processes because that used for I (i.e. molten phase filling [85]) is very different from that used for Cs (ion bombardment [90]), whereas the former is similar to that used for Bi [11] and Se [14,66] among others. The existence of some commensurability between the atom chain periodicities and the surrounding, curved graphene lattice was first proposed in [8] that could provide the driving force for generating the helical, single atom chains as the configuration of lesser energy. This was, however, not confirmed by further studies [9] and the aspect has not been investigated for Cs chains. The commensurability-related explanation should therefore be reasonably considered as a mere possibility so far. For untwisted periodic crystallites formed within MWCNTs, they cannot be directly commensurate with the innermost SWCNT if the conformation of the latter is chiral (i.e. not zigzag or armchair) [49] and can only be truly commensurate if the crystal periodicity matches that of the encapsulating armchair or zigzag nanotube or is some integral multiple of them.

5a.2.4.4 Compounds (as Nanowires or Nanoparticles)

Filling SWCNTs with compounds is a very important topic likely to provide successful alternatives when filling with chemical elements is not possible, typically because of too high a melting point and/or surface tension of the considered elements at the molten state (see Table 5a.1). Considering compounds may also give access to filling via solutions, as an alternative when a low-temperature filling process is needed or when the elements considered are poorly soluble. Compounds are typically salts, among which halides are the most popular, for the several advantages they offer such as high versatility (many types of halides are possible, that is, involving Cl, I, Br, or F, thereby offering a wide range of melting temperatures and solubilities); suitable range of melting points (i.e. not too high, e.g. < 1000°C) in many cases; good solubility in usual solvents (chloroform, water, etc.); and high chemical reactivity toward carbon that allows the nanotube to be opened and then filled by the molten halides all at once.

One of the most active groups involved principally in filling SWCNTs with inorganic materials has been based in Oxford although this is now been carried out by many other groups around the world. First, based on previous works on filling MWCNTs [60], SWCNTs have been filled with many kinds of halides and other compounds since 1998 [10], mainly using the melting method, but also using the solution method and, in a few instances, the gas phase route. The following list mostly corresponds to the materials inserted in SWCNTs (or DWCNTs) as reported by this group in the references provided (including review papers [37,123–125]), and includes an increasing number of materials inserted by other groups also. The list is likely incomplete, but provides an idea of the extensive work carried out in the field: HgTe [27], MnTe2 [126], (Na/Tl/Cs/Ag)Cl [37,125,127], (Cd/Fe/Co/Pd)Cl_2 [37,61,125,127], Ln(La to Lu)Tb/Ru/Ho/Gd/Au/Ag/Y/Fe]Cl_3 [10,20,25,61,83,88,121,127, 129], Al_2Cl_6 [37], (Hf/Th/Zr/Pt)Cl_4 [65,75,124,127], $MoCl_5$ [88], WCl_6 [37], $(KCl)_x(UCl_4)_y$ [82,85], CsBr [37], $AgCl_xBr_yI_z$ [48,82,85,130,131], (Li/Na/Cs/K/Rb/Ag/Cu)I [18,23,48, 123,131,132,133], (Ca/Cd/Co/Sr/Ba/Pb/Hg)I_2 [26,28, 123,127,134] (Te/Sn)I_4 and Al_2I_6 [37,129].

From 2001, oxides were also directly inserted into SWNTs, starting with CrO_3 [18,119] and Sb_2O_3 [135,136] and then followed by others such as PbO [84], Re_xO_y [67], and UO_2 [137] (although the latter was obtained from the primary filling of uranyl acetate) and hydroxides (KOH and CsOH [137]), sometimes with a fairly high filling rate (e.g. 80–90% for PbO). Although oxides can be interesting alternatives as intermediate compounds or can exhibit interesting intrinsic properties on their own (e.g. CrO_3 is electrically conductive), they will never become as popular as halides because oxides with high solubility in harmless solvents or reasonable melting temperatures are not many. Other popular compounds that were attempted for filling SWCNTs are typically nitrates, for example, silver nitrate [75,119,120], bismuth nitrate [11], uranyl nitrate [137], and so on.

Figures 5a.7 and 5a.8 provide examples of filling achieved with or via such compounds, respectively. In the case of Figure 5a.7, elemental Ag was initially introduced as the corresponding nitrate dissolved in water, while $GdCl_3$ and $HoCl_3$ (Figure 5a.8) were inserted from the corresponding molten salt.

5a.2.5 Filling Mechanisms

Data regarding physical properties of hybrid SWCNTs have now started to be reported, which is the most exciting part of this research field (see Section 5a.3). This should not suggest that synthesis mechanisms are well understood yet, specifically regarding filling via liquid routes although the work by Dujardin et al. [39,40] clearly indicates that the surface tension of the liquid used to fill nanotubes is as a key determinant for successful filling. However, because the pressure difference that makes a liquid enter and proceed within a tube is proportional to the liquid surface tension and inversely proportional to the tube diameter, according to a relation obtained by combining Young-Laplace's laws and Jurin's law [138], narrow tubes should fill over a longer length range than large tubes, meaning higher filling efficiency. However, this is not consistent with the conclusions from early works dealing with filling nanotubes with liquids, while comparing MWCNTs with a narrow and wide inner cavity, respectively. Indeed, until 1999, the filling of SWCNTs was estimated to be inefficient [39,139], and Ugarte et al. [38] actually stated that 'there appears to be a preference for the wider cavities to fill compared with the narrower cavities.' This

suggested that the laws (such as Young-Laplace's laws) driving regular (macro)wetting phenomena that were established for sub-millimetre capillaries could not apply to capillaries in the nanometre range ('nanowetting'). This was further supported by early predictions [140] who calculated that increasing the tubule radius decreases the incarceration energy and the overlap repulsion activation barrier at the mouth of the tube, from which it was deduced that material encapsulation in narrow SWCNTs via liquid or gas routes should be not be favoured with respect to larger MWCNTs.

However, actual experiments carried out on SWNTs were found to contradict such early statements based on MWCNTs. We did observe that filling efficiency appeared often better for regular SWCNTs (inner cavity ~1.4 nm on average) than for MWCNTs (inner cavity ~30–40 nm on average, herringbone type) for molten materials such as $GdCl_3$ and CoI_2. Likewise, condensation of Se was found to occur first in the narrowest nanotubes [66] and filling with Bi via the gas and liquid routes was found to be more efficient in SWCNTs than in MWCNTs 'as a result from stronger capillary forces' [11]. Generally speaking, SWCNT filling rates as high as ~70% (PbI_2 [28] and KI [82]) or even 80–90% (for PbO [84]) were observed and we can therefore conclude that nanowetting is a reality.

However, chances are high that discrepancies may occur in nanowetting with respect to regular macrowetting. For instance, it is reasonable to admit that there should be a minimal tube diameter below which filling is no longer possible. In macrowetting, molecules from the liquid located at the liquid/solid interface go slower than molecules from the liquid core, somehow inducing a convection-like effect at the progression front where friction-affected molecules are continuously replaced by unaffected molecules, which thereby feed the liquid/solid interface as the liquid progresses within the tube. In nanowetting, there should be a nanotube diameter below which the friction forces may affect all of the molecules of the liquid because they all can be considered as surface molecules, thereby preventing convection-like effects from occurring, thereby hindering filling. However, giving such a threshold value cannot be given because it also depends on the surface tension of the liquid material used to fill the nanotubes, for example, 4 nm for molten Al_2O_3 and 0.7 nm for molten V_2O_5 [38]. This might explain why extensive filling studies on SWCNTs have demonstrated that there is no direct relation between surface tension and filling efficiency [82]. In addition, as opposed to macrowetting, gravity is certainly not to consider in nanowetting because of the tiny volumes of liquid involved that make related weights negligible with respect to capillary forces. On the contrary, the role of viscosity, which is independent from surface tension (Hg provides a good example of a low viscosity liquid, 1.53 cP, with high surface tension of 490 mN m^{-1}), is likely to be enhanced in nanowetting. In macrowetting, viscosity is considered to only affect the wetting dynamics. The reason is, whatever the tube diameter, friction forces increasingly oppose the wetting forces because the tube/liquid contact surface where the friction forces take place increases as the liquid proceeds in the tube, while the gas/liquid/solid contact line where the capillary forces take place remains constant. This may ultimately cause the liquid progression to stop.

It is likely that viscosity and/or nanowetting are not the only criteria to consider for controlling the filling of nanotubes. The size of the atoms or molecules in the liquid, for instance, certainly matter for nanotube cavities below ~1 nm, specifically considering the solution method where the molecules to fill the nanotube with are surrounded by solvating molecules. In addition, the intrinsic saturating vapour pressure value of the desired filling

materials is likely to be important when using the molten phase method. Despite the filling temperature being maintained below the vaporization temperature of the filling material, some vapour pressure actually develops in the sealed ampoule. This pressure is likely to help the molten material to enter the SWNT cavity, with the consequence that materials with higher saturating vapour pressure should provide higher filling rates (considering that other parameters are equal). Such an aspect has not yet been investigated. Finally, local conditions may play an important role as well, as probably the only reason why, within the same filling experiment, some nanotubes are found extensively filled, whereas neighbouring ones are found empty, yet obviously wide open (Figure 5a.7(a)).

5a.3 Behaviours and Properties

As reminded above, the synthesis of X@CNTs, specifically involving SWCNTs, has a rather young history and examples of experimental measurements showing the peculiar properties of filled SWCNTs are still relatively few. Likewise, little theoretical work to tentatively predict the electronic properties of X@CNTs (excepting peapods) has been carried out thus far and expectations are mainly based on the anticipated possibility to modulate the SWCNT band gap thanks to the filling material, or to modulate the band gap of the latter thanks to the enforced structural deformations. Yet a variety of filled SWCNTs have been modelled (e.g. filled with materials as varied as KI [141], $(Sc,Ti,V)_8C_{12}$ carbohedrenes [142], water [143], DNA [144], Cu [145], Ag and CrO_3 [32], acetylene [146], Ge [147]), a majority of theoretical works mostly concerns transition metal filled SWCNTs, more specifically Fe, and aims at predicting the related magnetic behaviour with respect to the iron wire structure [148,149–152].

5a.3.1 Peculiar in-Tube Behaviour (Diffusion, Coalescence, Crystallization)

Thanks to the unidirectional feature of the inner cavity in carbon nanotubes, specifically in SWCNTs, a variety of peculiar in-tube behaviours of the filling materials can be observed, which occur either spontaneously upon filling, or under the effect of an external stress (annealing, irradiation…).

Several interesting examples can be found with peapods, whose some are given below, that will be further commented in Chapter 5b. When subjected to an electron beam in a TEM, fullerenes encapsulated in SWCNTs have actually shown a series of peculiar behaviours including diffusion [153], dimerization [46,153,154] and coalescence [154]. Such behaviours were specifically permitted by the encapsulated situation of the fullerenes because no such behaviour was observed for fullerenes in bulk fullerite (i.e. nonencapsulated) when electron irradiated. The former (fullerene diffusion) requires the filling of the SWCNTs to be partial only, in order to leave the room for observing the phenomenon. It is illustrated in Figure 5a.11. Another example can be found in [13].

On the contrary, the two latter (dimerization and coalescence) require the fullerenes to be densely packed. They are illustrated in Figure 5a.12. Briefly, irradiated fullerenes tend to first get closer to each other in pairs, assuming dimerization (Figure 5a.12(b)), and then to coalesce into elongated, somewhat distorted capsules (which may be regarded as higher, elongated fullerenes).

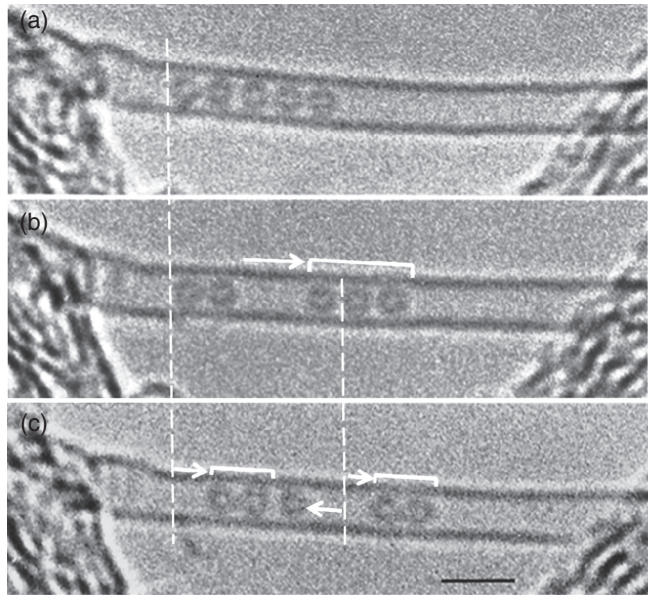

Figure 5a.11 *Sequence of high resolution TEM images (100 kV, ~10 seconds between images) illustrating the irradiation-promoted diffusion of the encapsulated fullerenes within a SWCNT (the 'nanoshuttle'). (a) Starting situation, showing an ensemble of five fullerenes. (b) The five fullerenes suddenly split into an ensemble of three fullerenes which move to the right, leaving behind an ensemble of two fullerenes. (c) One fullerene from the ensemble of three moves back to join the former ensemble of two and leaves another ensemble of two. Meanwhile, both the ensembles of two have slightly moved to the right. All the moves are presumed to be ionization-driven, explaining why they are random and either repulsive or attractive (depending on whether electrons are captured by or taken from the fullerenes). Modified with permission from [103] Copyright (2003) American Physical Society.*

Chapter 5b will show that fullerene coalescence may also occur upon several other kinds of treatments, including thermal annealing [103,155], combinations of thermal annealing and electron irradiation [56,156,157] and photon (laser) irradiation [158,159]. Thermal annealing goes in the direction of thermodynamic stability and ultimately can result in the destruction of the tubular morphology then transform the whole peapod material into a graphite-like material. On the other hand, irradiation combines thermal energy supply and ballistic damaging which ultimately can be destructive to the tube. Hence, depending on the amount of energy supplied and the way it is supplied (e.g. by temperature, or situations of resonance upon laser irradiation), the coalescence process can produce elongated capsules, an inner SWCNT (thereby making a DWCNT), a polyaromatic material, or amorphous carbon.

Low-dimensional crystals formed within SWCNTs do not undergo quite the same types of structural transformations which are described in the previous section for peapods. Related dynamic behaviours upon electron irradiation have however been reported for other materials encapsulated in SWCNTs such as clusterization of $ZrCl_4$ crystals [65] and the observed steady rotation of Re_xO_y clusters [67]. The former (clusterization) is distinct

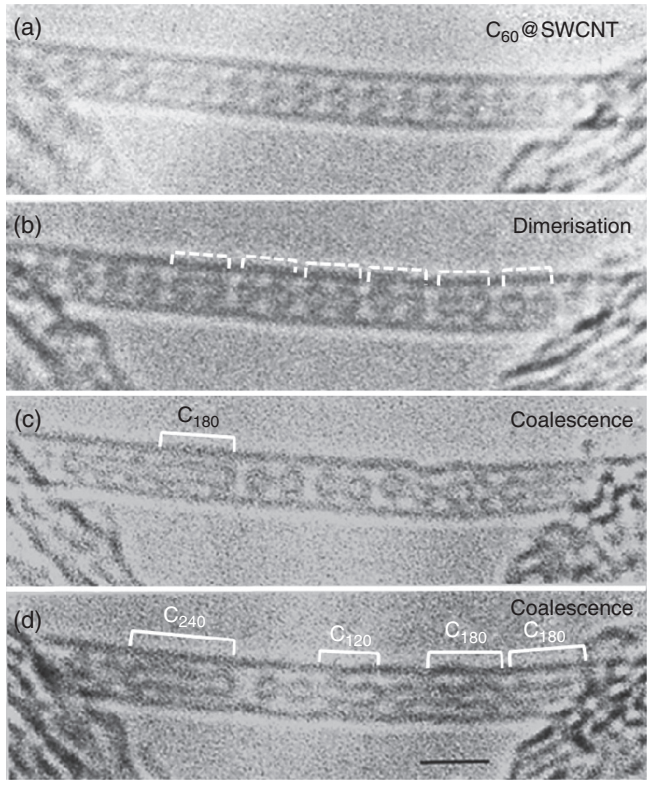

Figure 5a.12 *Sequence of high resolution TEM images (100 kV, ~300 s between images) showing the progressive coalescence of C_{60} molecules to higher fullerenes as elongated, distorted capsules under the effect of electron irradiation, starting from a regular C_{60}@SWCNT peapod. (a) Starting situation, exhibiting a well periodic display of the fullerenes. (b) Dimerization occurs first, making the C_{60} get closer by pairs. (c) Coalescence starts, yet not uniformly. (d) Coalescence proceeds, which may make the formerly formed elongated capsules merge as well. Modified with permission from [154] Copyright (2000) Elsevier Ltd.*

from the progressive agglomeration that was described for fullerenes, as instead we see an effective breaking down of a local crystal structure, whereas the latter (cluster rotation) is commonly observed for both types of encapsulates formed within SWCNTs.

In addition, the mere fact that encapsulating crystals in SWCNTs enforces a nanowire morphology that is generally unusual for most of the filling materials tested thus far is intrinsically a peculiar behaviour, as demonstrated by attempts to remove the carbon sheath, which resulted in the loss of the nanowire morphology for several halide crystals [48]. Moreover, a second major behaviour that is specific of the encapsulation in SWCNTs is to frequently generate often profound structural modification for a material with respect to the same material as it is observed in the bulk state. Structural crystallographic peculiarities actually include preferred orientation with respect to the nanowire elongation axis, systematically reduced coordination, lattice expansion and/or contraction, and, occasionally,

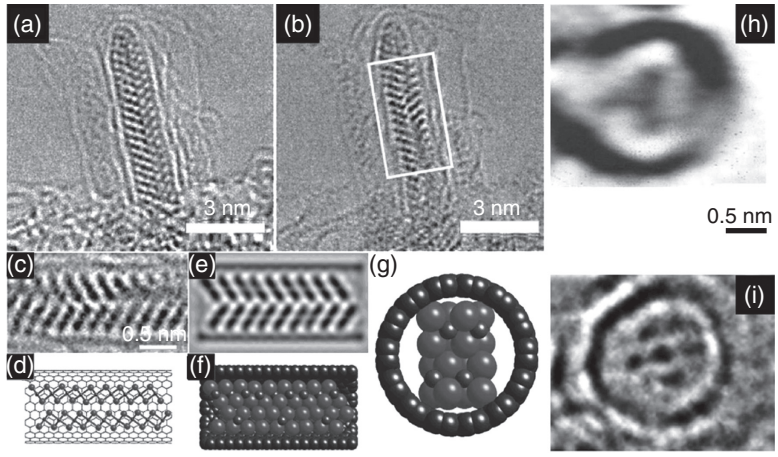

Figure 5a.13 *(a) and (b) High-resolution TEM images of a tip of a SWCNT filled with PbI_2 for two different focus values of the objective lens. (c) Enlarged image of the area framed in (b). (e) Corresponding calculated image, based on the model in (d). Although bulk PbI_2 structure is a two-dimensional layered type, encapsulation in SWCNTs enforces it to become a one-dimensional polyhedral chain. (f) and (g) Ball and stick models of the structure modelled in (d), as a side and a cross-section views respectively. (h) High-resolution TEM image of a cross-section of a SWCNT filled with CrO_x. The filling material structure exhibits a three-fold symmetry in which each lobe is assumed to be the projection of a chain of CrO_4 tetrahedra (reprinted with permission from [18] Copyright (2001) Elsevier Ltd). (i) High-resolution TEM image of a cross-section of a SWCNT filled with $HoCl_3$. The filling material structure exhibits a somewhat five-fold symmetry, yet is deformed. Based on the observed structural similarities with $NdCl_3$ [24], each dark spot is assumed to a projection of a single 1D chain of $HoCl_x$ polyhedra. For a better understanding of the figure, please refer to the colour plate section.*

new crystal structures. Preferred orientation may originate from the need to maintain the stoichiometry as far as possible, in the case of binary or higher order compounds [123]. Reduced coordination is obviously a consequence of the sterically confined space in which the encapsulated crystals have to grow, which may also be the cause for the lattice expansion in the radial direction as observed for CrO_x [18] and KI [22]. Lattice distances along the wire axis are less likely to overcome distortions because the confinement is relatively nil in this specific direction but numerous examples of a lattice contraction in this specific direction can be found, for example, KI, [23] Sb_2O_3 [135,136] and even fullerenes because the 1 nm C_{60}-C_{60} distance in fullerite was found to become 0.97 nm for C_{60} chains in peapods [160]. Such lattice contraction behaviours correspond to the Poisson effect, which is well known in bulk material mechanics. Such lattice distortions are significant, and may reach 14% or more. Despite the crystallization of binary halides may adopt different structures (three-dimensional, layered, chain and molecular in bulk state) [161], it is clear that the limited space available in SWCNTs (and DWCNTs) will not allow all of them to develop (specifically for the three-dimensional and the layered structures), depending on the radius of the atoms involved (Figure 5a.13 (a)–(d)). Interestingly, a recent study [162] showed that in wide inorganic nanotubes based on WS_2, not only does the layered

iodide PbI_2, introduced from the liquid phase, revert to its bulk structure type but this distorts in order to allow the encapsulated iodide to form core-shell nanotube structures, forming in effect tubes within tubes, inside the WS_2 capillaries. It is interesting to speculate that similar structural behaviour might be observed for wide nanotubes based on carbon although this is yet to be reported.

For a given compound, the structure type may change with respect to the available inner space within the nanotube capillaries [28,37,124,134]. Ultimately, structural constraints can be such that new structures are created, for example, for $HoCl_3$ [13], CrO_3 [18], $NdCl_3$ [24], CoI_2 [26], or BaI_2 [134], giving rise to peculiar features such as unusual symmetry (Figures 5a.13(h),(i)). Finally, it was observed that the ability of the filling material to crystallize may depend on the available inner space on the one hand, and on the deformability of the tube wall on the other hand. Indeed, small diameter SWCNTs were found to accommodate the contained crystal structure (CoI_2 [26] or PbI_2 [28]) to such an extent that the host SWCNTs exhibit oval cross-sections. Accordingly, PbI_2 was found to be amorphous when filling DWCNTs with similar small diameter, presumably because the deformability of the tube wall is much decreased, hence not allowing the crystal structure to develop.

Molecular dynamics (MD) simulations which are based on interatomic and intermolecular forces rather than specific electronic interactions are also proving to be very useful tool for both interpreting and predicting filling behaviour. Indeed, this has been prominently applied to ab initio predictions of the crystallization of water within nanotubes [34,35]. Wilson and Madden [141] have used such an approach to model the crystal growth behaviour of KI in variable diameter SWCNTs using such an approach. The interactions between the ionic K^+ and I^- species were described by standard Born–Mayer pair potentials with the assumption that the ions retained their formal integer charges. Interactions between the ions and the walls of nanotubes of varying diameters were described by Lennard–Jones potentials, with parameters derived from potentials for the interactions of isoelectronic inert gas atoms with the carbon atoms of the graphene surface. Time-resolved and minimum energy simulations predicted the filling of (10,10) SWCNTs with thermodynamically ordered arrays of 2×2 KI crystals starting from an open SWCNT immersed in molten KI. Minimum energy simulations also predict lattice distortions that were consistent with those observed experimentally. Wilson subsequently adopted a similar approach to produce in effect a 'phase diagram' of minimum energy versus observed structure type (Figure 5a.14(b)) [163]. As a result, a phase diagram could be constructed which predicts, in an ab initio fashion, the predominant structure type for the typical median range of nanotube diameters which form for SWCNTs. For diameter ranges of 1.1–1.3 nm and 1.6–1.8 nm, effectively $2 \times 2 \times \infty$ and $3 \times 3 \times \infty$ rock salt-type 1D KI crystal structures are predicted. Outside these ranges, other 1D crystal structures are expected. In the lowest diameter range studied (i.e. 1.0–1.1 nm), a so-called T3 structure is predicted, which is a twisted crystal structure in which the cross-section of the crystal consists of a three-membered ring (i.e. –I–K–K– or –I–I–K–). Similarly, in the ranges 1.3–1.35 nm and 1.47–1.55 nm, T5 and T7 twisted 1D crystal structures with five– (e.g. –I–K–I–K–I–, etc.) and seven– (e.g. –I–K–I–K–I–K–I–, etc.) membered rings formed in cross-section, respectively. In one range, from 1.35–1.47 nm, a so-called 'hex.' structure is formed in which the encapsulated structure can best be described in terms of a stacked 1D array of alternating six-membered shells of the form –I–K–I–K–I–K– and –K–I–K–I–K–I–.

Even more remarkably, this technique was applied by the same researcher to predict the formation of inorganic nanotubes within SWCNTs (i.e. a tube within tubes) [164]. Similar approaches were also adopted with regard to predicting both ice phase transitions within carbon nanotubes and also the formation of ice tunnels and crystals within the same (see Figure 5a.15 (a)–(d)) [34,35]. In an extension to the KI modelling work, both chiral and achiral inorganic nanotubes form within SWCNTs according to the ambient nanotube diameter (Figure 5a.15(e) and (f)). What made this work particularly remarkable is that it successfully predicted the formation of a later observed nanostructure, HgTe in SWCNTs (see Figure 5a.15(g)-(n)) [27].

5a.3.2 Electronic Properties (Transport, Magnetism and Others)

The structural features described above provide good prospects that some hybrid SWCNTs should exhibit quite peculiar physical properties, specifically regarding transport and magnetism. As far as properties are concerned, the distinction should be made between (i) the peculiar behaviours of the filling materials specifically resulting from their encapsulation; (ii) the properties intrinsically from the filling materials that are naturally transferred to the whole hybrid nanotube; (iii) and the peculiar properties that may result from the nanotube/filling material interactions. With respect to filled MWCNTs, case (iii) is not to be expected because the interaction, if any, can barely affect more than the innermost graphene and the properties of the multi-graphene wall are dominated by that of the polyaromatic layer stacks. Case (i) is not impossible but seldom because, as already pointed out in the *Introduction* section to the chapter, the inner cavity is often too large for the confining conditions to be significantly stressful to the filling materials, leaving little chance for peculiar properties. Case (ii) is actually more likely and one example of it is the filling with ferromagnetic material, making the whole hybrid CNTs ferromagnetic as well.

Hence, the investigations of filled CNT properties have focused on filled SWCNTs rather than filled MWCNTs. Unfortunately, such examples are still relatively few. Probable reasons are that although high filling rates can be achieved that are suitable for structural investigation, the whole material may remain too imperfect (e.g. impurity content) to investigate them as a bulk in a reliable manner. On the other hand, investigating isolated, single X@CNTs requires nanolithography facilities and specifically-designed measurement devices that are not of common and easy access yet. In addition to possessing the related technological knowhow, explaining and understanding the phenomena observed requires one to be able to characterize the very same X@CNT tested to ascertain the extent of filling and the structural features of the encapsulating SWNT, which is definitely not routine.

Again, most of the work published thus far deals with peapods and related materials and has addressed issues related to thermal properties [165], transport and charge transfers (between the encapsulated materials and the containing SWCNT) [95,100,165–172]. Those aspects will be presented in Chapter 5b.

Less abundant in literature, other interesting and promising observations have been made on SWCNTs filled with materials other than fullerene-related. As early as in 1998, the electrical resistivity of I@SWNT was found to be significantly decreased with respect to pristine SWNTs, with some evidence for charge transfer [86]. However, it is difficult to ascertain that this result accounted for the contribution of encapsulated iodine, because iodine *intercalation* (i.e. of I atoms in the interstitial spaces between hexagonally packed SWCNTs within bundles and also in the spaces between bundles) certainly occurred as

well. It is not a trivial issue to question whether I doping in interstitial sites and within capillaries contribute similarly because both sites do not necessarily 'see' the same graphene curvature and different electronic interactions may therefore result. Interactions between foreign materials other than iodine for which the filling position is ascertained and the encapsulating SWCNT is, however, demonstrated, resulting in, for example, charge transfer (with Ag and CrO_x [32], AgCl [128]), reduction of band gap (with $MnTe_2$ [126]), energy transfer modifying the optical adsorption range (with squarylium dye) [7].

At this stage, it is certainly useful to consider first principles ab initio density functional theory (DFT) calculations and, in this regard, some very useful work is starting to be done. In the case of filled SWCNTs formed between $M(\eta\text{-}C_5H_5)_2$ where M = an early transition metal (i.e. Fe, Co), first principles density functional pseudo-potential calculations were used to investigate the nature of interactions between 'flat' graphene, SWCNT, and the intercalated metallocene complex [173]. A further variable considered was also the respective diameter and structural conformation of the encapsulating nanotube. The obtained results demonstrated that the composites were stabilized by weak π-stacking and CH ↔ π interactions, and, in the case of the $Co(\eta\text{-}C_5H_5)_2$@SWCNT composites there is an additional electrostatic contribution as a result of charge transfer from $Co(\eta\text{-}C_5H_5)_2$ to the nanotube. The extent of this charge transfer was rationalized in terms of the electronic structures of the two fragments, or more specifically, the relative positions of the metallocene highest occupied molecular orbital (HOMO) and the conduction band of the nanotube in the electronic structure of the composite. The study concluded that control over the electronic properties of specific SWCNTs, which have been selected from the bulk according to the nanotube diameter and/or chirality, might be achievable via the non-covalent modification of SWCNTs by neutral and charge transfer molecules. Experimentally, this kind of transfer had previously been observed by a combination of optical absorption and Raman spectroscopy [5] so this type of synergy between theory and experiment is clearly valuable.

In this regard, modelling has certainly shown to be useful to understand hybrid SWCNTs well and to support experimental measurements. Such a consistency is claimed for Ag- or CrO_3-filled SWCNTs, whose modelling confirms to the donor and acceptor roles, respectively, of the filling materials toward the containing SWCNTs in agreement with the resonant Raman data [32]. Electron transfer was also found in bulk ferrocene@SWCNT material upon photoexcitation [105]. However, the recent work by Carter et al. [27] can be considered the first full demonstration of the modification of the electronic behaviour (namely, the change from semimetal to semiconductor) from the geometric constrains imposed on the encapsulated crystal in a HgTe@SWNT material. It was subsequently noted [174] that the observed new structural form of HgTe in which Hg is in trigonal coordination and Te is in half-octahedral coordination [27,174] is effectively isostructural with the new form of inorganic nanotube predicted by Wilson (see Figure 5a.15 (e)–(n)) [164]. Recent DFT work by Yam et al. [175] Sceats et al. [176] and also Christ and Sadeghpour [177] has also been applied to the KI@SWNT system and all demonstrate a clear tendency for, in particular, the 2 × 2 inclusion to promote metallic behaviour in the encapsulating nanotube principally as a result of charge transfer. The recent apparent observation of Lindqvist ion expansion in DWCNTs [118] also offers intriguing possibilities for studying the structural response of polyoxometalates to charge transfer between the filling material and the containing nanotube.

The magnetic behaviour of filled SWCNTs is also a fast-growing topic, although theoretical works [145,149–151] are still more numerous than experimental ones [12,121,122,178].

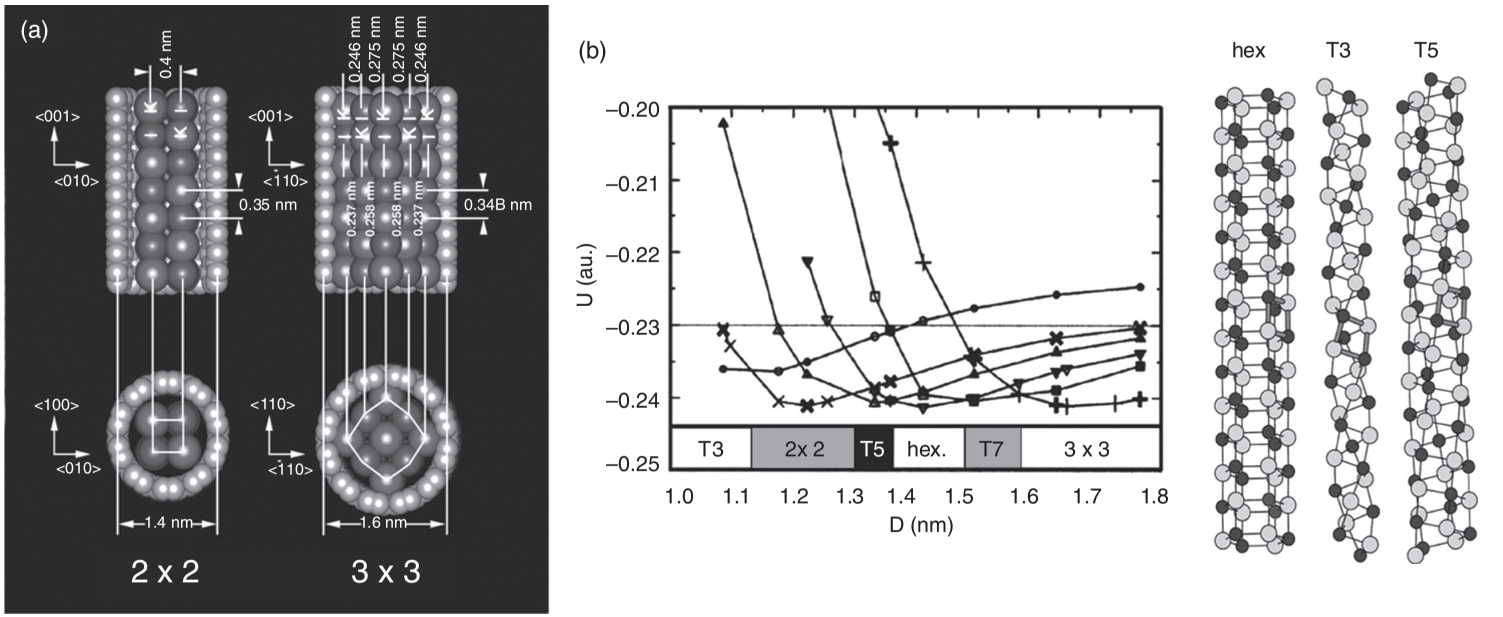

Figure 5a.14 *(a) Structure models of 2 × 2 and 3 × 3 layer KI@SWCNT hybrid nanotubes determined experimentally. (b) Minimum energy (U) phase diagram depicted for structure types of KI predicted to fill SWCNTs of varying diameter (D). T3, T5 and T7 are helical KI 1D crystals with three-, five- and seven-membered rings in cross-section, respectively. For a better understanding of the figure, please refer to the colour plate section. Reprinted with permission from [163] Copyright (2002) Elsevier Ltd.*

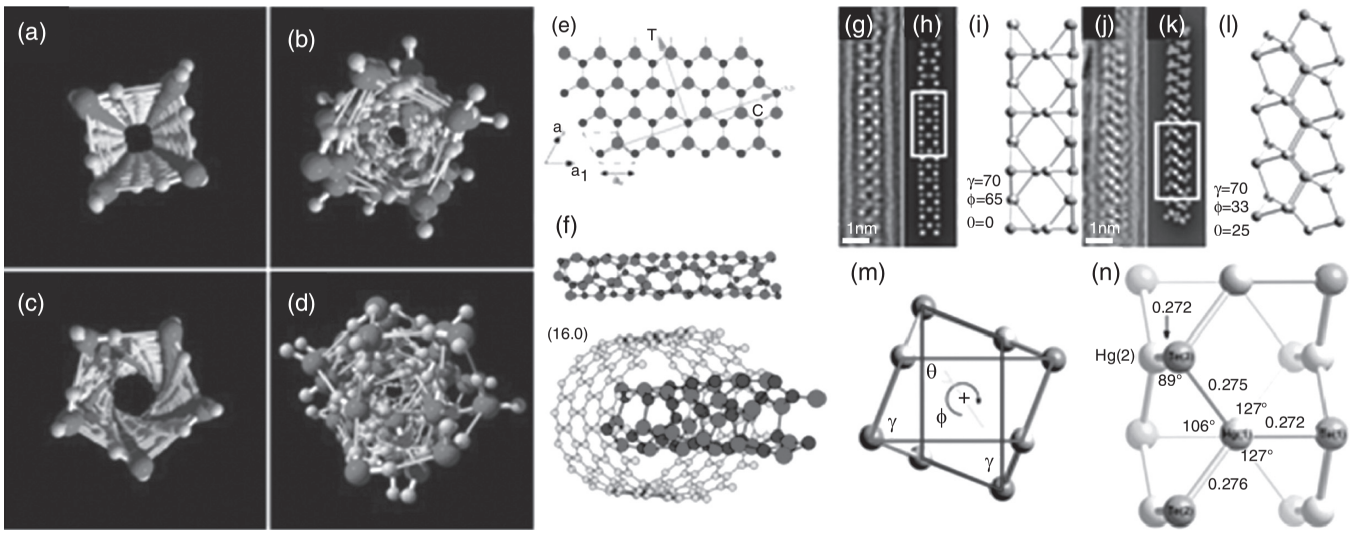

Figure 5a.15 *(a) and (b) Square and hexagonal ice tunnels formed within (14,14) and (15,15) SWCNTs respectively. The containing SWCNTs are not shown for clarity. (c) and (d) show the corresponding liquid phases, respectively (reprinted with permission from [34] Copyright (2001) Macmillan Publishers Ltd). (e) to (f): The construction of an inorganic nanotube from a corresponding hexagonal planar structure. The red and blue circles represent the two ionic species. C_h is the chiral vector along which the structure must be folded in order to form a (3,2) hexagonal nanotube. The bottom sketch in (f) shows a perspective view of a (3,2) inorganic nanotube within a (16,0) SWCNT. This nanostructure turned out to be nearly identical to a similar nanostructure later reported within a SWCNT by HgTe [27]. (g), (h) and (i) show a reconstructed phase image, corresponding image simulation, and structure model respectively, of one projection of a twisted, chiral HgTe crystal in a SWCNT. (j), (k) and (l) show similarly a phase image, simulation, and model from a second twisted HgTe crystal in a separate carbon nanotube. (m) and (n) show the end on views of the essential structure motif and corresponding DFT-optimized model corresponding to the materials shown above them respectively. There is a close correspondence between this model and the model shown in (f)(reprinted with permission from [164] Copyright (2004) Elsevier Ltd). For a better understanding of the figure, please refer to the colour plate section.*

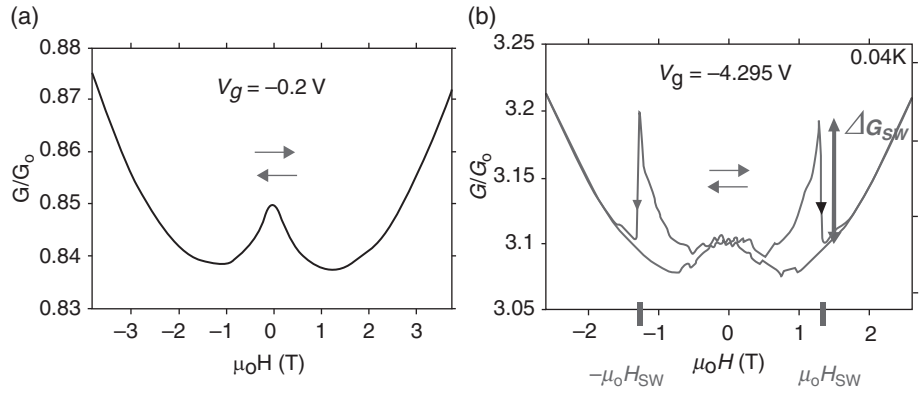

Figure 5a.16 *Variation of conductance versus cycling magnetic field measured on individual Co@SWCNT bundles contacted (with Pd) following the transistor-type device, for an angle of 25° between the direction of the outer magnetic field and the elongation axis of the contacted bundle, and at a temperature of 40 mK. (a) 90% of the devices do not show a hysteretic behaviour, as illustrated, whatever the gate voltage. (b) 10% of the devices show a hysteretic behaviour, as illustrated. Conductance curves indeed exhibit a hysteresis with two conductance jumps. They correspond to the magnetic field value at which the magnetization direction of a nanomagnet (presumably one, or several but aligned, encapsulated cobalt wire segment(s) reverses (reprinted with permission from [179] Copyright (2011) American Chemical Society). For a better understanding of the figure, please refer to the colour plate section.*

The latter examples showed that, for iron, the ferromagnetic property is maintained in spite of its nanowire morphology with a nanometre-sized diameter, as a good example of an intrinsic property of the encapsulated material that is transferred to the whole hybrid material. Interactions between the magnetic filling material and the encapsulated SWCNT are also possible, as recently demonstrated with Co@SWCNT materials contacted according to a transistor-type device, which showed the occurrence of magneto-resistance effects when operated at temperatures close to absolute zero in cycling magnetic field conditions (Figure 5a.16) [179]. It is also worth noting that, in the same material, the main direction of magnetization was found to be perpendicular or oblique to the elongation axis (as opposed to what was found for large Co wires encapsulated in MWCNTs [180]), as a direct consequence of the high proportion of surface atoms in the encapsulated Co nanowire whose radial dimension is minimized due to the narrow diameter of the containing SWCNT [179].

5a.4 Applications (Demonstrated or Expected)

5a.4.1 Applications that Make Use of Mass Transport Properties

5a.4.1.1 Filtration

Current studies on mass transport are principally concerned with using carbon nanotubes as a filter for processing gases and molecules (i.e. either in the gas phase or in solution) through permeable membranes in which embedded nanotubes provide the pores through

which these species are filtered [181]. As indicated in previous sections, gas/liquid transport is the principal mechanism whereby materials are introduced into nanotubes. In one sense, however, this section does not really belong here as we are actually more interested in the properties of the kind of nanocomposites that filled nanotubes actually are, rather than in nanotube pipes through which liquids or gases transit and which obviously are not nanocomposites. But these studies are worth noting in this context because they are useful in terms of giving further guidance as to the limitations of nanotube inclusion as a function of tube diameter because this is clearly both a sterically controlled phenomenon and also one which is closely controlled by the physical smoothness (or potential energy surface) of the host nanotubes. In practical terms, we should also note that this field has undergone considerable development in recent years.

Various researchers have undertaken significant investigations into the transport properties of various gases and solutes through SWCNT membranes. Johnson and Scholl (and coworkers) for example [181], have studied processes such as the absorption and diffusion of CO_2 and N_2 through SWCNT membranes [182] and also the rapid transport of H_2 and CH_4 through SWCNTs [183] Similarly, Hinds et al. [184] have produced results on the transport of N_2 gas and $Ru(NH_3)_6^+$ in solution through aligned MWCNT membranes and Holt et al. [185] have studied the diffusion of a variety of gaseous species including H_2, He, N_2, O_2, Ar, CO_2 and the hydrocarbons gases including CH_4 (smallest) and C_4H_8 (largest) through aligned DWCNT and MWCNT membranes. The significant theoretical work is probably that of Johnson's and Scholl's team which reveals that the inner potential energy surface of carbon nanotubes, to a very good approximation, makes them behave like atomically flat cylinders that easily permit the flow of molecules through their inner capillary channels. Interestingly, they also comment: 'We have considered only defect free nanotubes in our calculations. The presence of defects in the nanotubes (heteroatoms, holes, etc.) may have a profound effect on molecular diffusion by adding corrugation to the molecule-solid potential energy surface.' In fact, nanotubes themselves are corrugated even without this consideration, and it is enough to look at STM studies such as in [188] (and references therein) to see this. Also, none of the works cited above but one [185], addresses the limiting case where the diffusing species is sterically similar (i.e. almost the same size) to the internal volume of the nanotube; nearly all the molecular species addressed (i.e. CO_2, N_2, H_2, CH_4 and $Ru(NH_3)_6^+$ etc.) are significantly smaller than the internal van der Waals surface and are therefore 'free' to diffuse through the nanotubes. The notable exception is the work by Holt et al. [185] which describes the transport of a variety of gaseous species performed with sterically matched gold colloids and one large molecular species $Ru^{2+}(bipyr)_3$ which were used to estimate the diameter of the pores of the nanotubes making the 'holes' in their permeable membranes. As the authors themselves stated, these studies provided them with an estimate of the average pore size (for example, their membranes fabricated with aligned DWNTs were estimated to have pore sizes between 1.3–2 nm based on the fact that they exclude most gold colloids with a diameter of 2 nm: +/– 0.4 nm) but this study provides some very interesting insights into how nanotubes falling within a certain diameter range can accommodate species of a particular size.

In summary, such studies provide two useful additions to a consideration of the properties and applications of filled nanotubes: (i) they give us very clear indications as to the steric properties of nanotubes and therefore give us semiquantitative information on

how they are able to discriminate and/or accommodate species of a particular size to fill them with; (ii) in the potentially important area of drug or substance delivery (see next), such diffusion studies give us important indicators as to how effective nanotubes are likely to be in this role.

5a.4.1.2 Targeted Molecular Species Delivery (Biomedical Applications and Others)

Further to the foregoing discussion, several researchers have proposed filled carbon nanotubes as vehicles for the delivery of bio-active agents for medical applications, because of the overall biocompatibility of graphene. The related works deal with the potential of nanotubes to be used in effect as:

1) Nanocontainers, to instil in the tissue then activate by induction, as with for example, iron [181,189,190] for magnetotherapy, which is used for the selective heating and destruction of diseased tissue (by the application of an inductive field). The filled nanotubes can also be opened after instillation to release their contained agent, for example, when filled with anticancer drugs such as carboplatin [191,192] and cisplatin [193] to initialize their medical virtue. In both cases, however, the molecular species to deliver does not really transit through the nanotubes but is delivered along with the nanotubes which are merely used as a vehicle. This makes that this application better pertains to the next Section 5a.4.2 but was placed here in order to merge all biomedical applications. Another biomedical application that uses CNTs as nanocontainers is to instil wherever is needed in the tissues contrast agents for medical imaging such as magnetic resonance imaging (MRI); when encapsulated in CNTs, those contrast agents, whose most popular ones are currently gadolinium-based compounds, have better chance of not interacting with the body as well as better chances of being eliminated from it. Gd-filled SWCNTs [194] as well as Fe_2O_3-filled SWCNTs [195] were successfully tested, with a dramatically enhanced imaging contrast resulting from the absence of any organic component and the enrichment of the magnetic atom (or compound) concentration.
2) Microcatheters [196] or nanopipettes [197–199], in which nanotubes are merely used as nanopipes. In truth, the latter was properly demonstrated only very recently [199] whereas most of studies until now have concentrated instead on the thorny issue of the biocompatibility of carbon nanotubes which have a tendency to promote in vivo cell coagulation (in this respect, the review presented in [196] is a typical example).
3) Applications related to that above should follow, such as nanoprinting: connecting a nanopipette to a reservoir of molecules whose diameter is small enough to diffuse freely within the nanotube cavity, should allow for the controlled and patterned deposition of the latter onto a surface. Using charge-bearing molecules and applying a potential difference between the printing head and the deposition surface might be necessary to actually extract the molecules from the CNT needle.

5a.4.2 Applications Arising as a Result of Filling

5a.4.2.1 Field Emission

One of the potentially most realisable applications of carbon nanotubes has been their use as field emitters. This is in part due to the comparative ease with which 2D arrays of carbon nanotubes can be grown on a flat or on a curved substrate. Because the nanotubes can be formed from catalyst metal islands whose positional and size distribution can be precisely

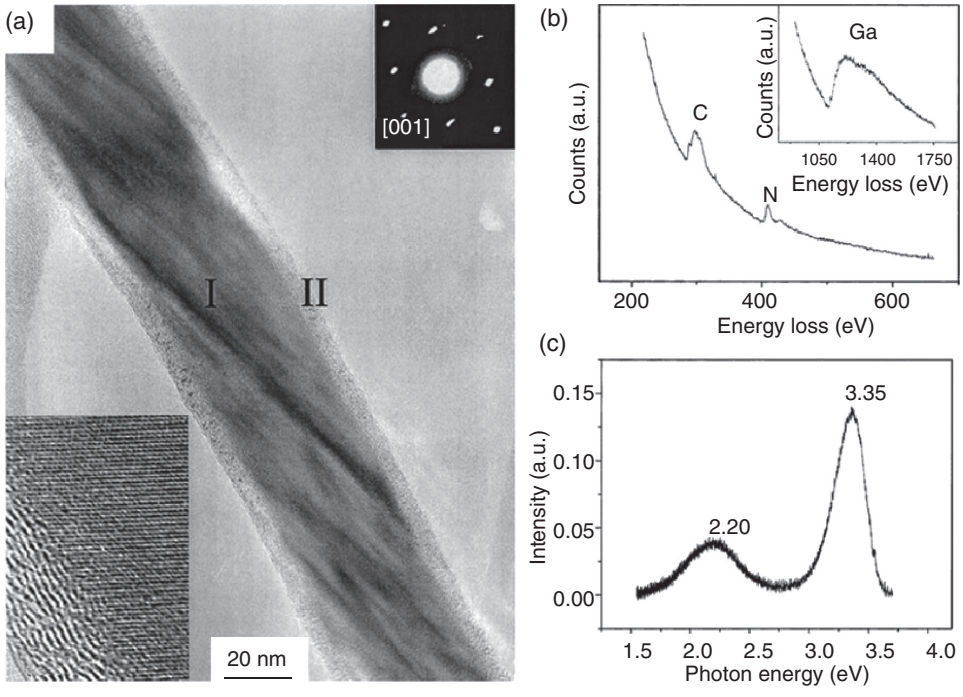

Figure 5a.17 *(a) TEM image of a GaN@MWCNT hybrid nanotube; bottom-left inset shows the well crystallized structure of the filling GaN (whereas the nanotexture of the containing MWCNT wall is rather low); top-right inset shows that the GaN filling actually makes a single crystal. (b) EELS spectrum showing that the chemical composition is only C (from the MWCNT) and N, and Ga (inset). (c) Photoluminescence spectrum of the GaN nanowires encapsulated in CNTs. Reprinted with permission from [200].*

controlled, producing carefully grown arrays is comparatively trivial. In addition, the atomically thin cross-sectional dimensions of nanotubes combined with their high aspect ratio and semiconducting/metallic character (i.e. according to conformation) makes them ideal candidates as field emitters in micron scale devices. An obvious enhancement to this application could arise if filling the nanotubes were to produce some obvious benefit with regard to enhancing the field emission properties. There are relatively few works describing the enhancement of such field emission apart from a brief communication by Liao et al. [200] describing the stable field emission from GaN filled nanotubes (Figure 5a.17) synthesized by a combination of catalytic growth and plasma enhanced deposition [201]. A close study was carried out by Domrachev et al. [202] who have also investigated the MOCVD synthesis and field emission characteristics of Ge-filled carbon nanotubes, but the containing nanotubes were made of a 'diamond-like' carbon material instead of genuine graphene-based carbon. At least one study has also described the field emission characteristics of an array of nanotubes filled with iron oxide [203] but, as with the GaN studies, this work has concentrated on filled MWCNTs rather than filled SWCNTs presumably due to the comparative ease of synthesis and also due to the relative mechanical stability of MWCNTs compared to SWCNTs during the electron emission process.

5a.4.2.2 Detectors

An area of considerable future potential may arise from the ability of nanotubes formed at the lowest dimension (i.e. SWCNTs and DWCNTs) to change or alter the crystallographic state of the filling material, as we have described above for a variety of filling materials, for example, CrO_x [18], BaI_2 [134], CoI_2 [26], and HgTe [27] in SWCNTs, and PbI_2 in DWCNTs [28]. In particular with the semimetal HgTe (with a band gap of -0.3 eV) it has been possible to show that encapsulating this material within SWNTs forces this structure into a new graphene-like crystallographic form which is now semiconducting (with a band gap of +1.3 eV) [27]. Similarly, PbI_2 is usually a wide but variable band gap semiconductor in the bulk (with a band gap of 2.2–2.6 eV) which is useful in the X- and γ-ray detection domain. The variability of the band gap is generally attributed to polytypism (2H, 4H and 12R stacking, etc.) which can be induced by kinetic heating of the halide in the bulk but which can only be healed with difficulty by careful annealing. Such a polytypism is sterically forbidden when the material is constrained within the capillaries of SWCNTs and DWCNTs which will similarly have the effect of constraining the band gap (and possibly also tuning it as a function of the encapsulating nanotube). These properties may lead to the development of these materials in detector applications.

5a.4.2.3 Catalyst Support

Other areas of interest have included the use of filled nanotubes as catalyst materials [60,204] or as catalyst support [205]. In the latter case, the nanotube is not only used, as usual, as a high surface area substrate for nanosized catalyst particles located at the nanotube outer surface (as reported in Chapter 4) but the synergetic confinement inside the MWCNTs of both the catalyst (Rh) and the fluids ($CO + H_2$) to convert (into ethanol) was shown to result into a formation rate exceeding by one order of magnitude that of the similar reaction carried out with the Rh nanoparticles located outside, instead of inside, the MWCNTs. This is quite promising for industrial applications, once cost issues related with preparing the nanotubes and fill them will be ruled out.

5a.4.2.4 Electrochemical Energy Storage and Production

Their use in electrochemical energy storage and production, in point of fact, was among the earliest suggested applications for filled nanotubes [60,204]. But related demonstrations are seldom, specifically when involving SWCNTs as the containing nanotubes. It is therefore worth noting the first demonstration of it, which also was the first demonstrated application for X@SWCNT materials, which involves CrO_x@SWCNTs as a material to build electrodes for symmetric supercapacitor devices capable of unprecedented charging speeds, thanks to Faradaic reactions that occur between the nanosized CrO_x crystals and the acidic electrolyte [206]. In this study, the material was not optimized for reaching high capacitance values, a work still to be carried out but Galvanometry curves was still showing the desired square-like profile even at scanning speed of 1 V s^{-1} (Figure 5a.18).

5a.4.2.5 Future Electronics

Finally, one of the most intriguing applications put forward for filled nanotubes, particularly those containing endofullerenes, is the idea that they may be used in single spin devices which may partly arise from the polarizing electronic properties of the encapsulating

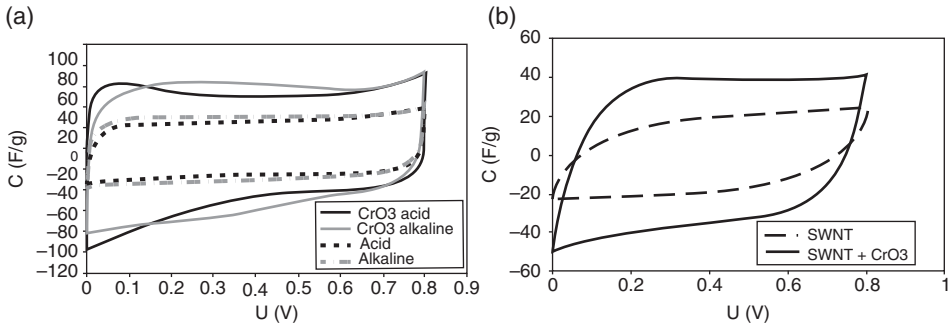

Figure 5a.18 *CrO_x@SWCNT materials were used as electrodes for a symmetric electrochemistry cell and the supercapacitor performances were measured by Galvanometry in either acidic or alkaline electrolyte, and compared to the same using pristine SWCNTs. The voltage was cycled from 0 to 0.8 V at various scan rates (from 0.002 to 1 V s^{-1}) while the capacitance was measured. (a) Whatever the electrolyte or the scan rate, using CrO_x@SWCNT (solid lines, labelled 'CrO_3') instead of pristine SWCNT (dashed lines) electrodes results in a capacitance gain. The irregular shape of the CrO_x@SWCNT-related curves indicates the occurrence of Faradaic reactions, which are believed to be responsible for pseudo-capacitance effects. The example shown is for a scan rate of 20 mV s^{-1}. (b) Remarkably, the desired square-like shape of the galvanometric curve is maintained with the CrO_x@SWCNT electrodes at a scan rate as high as 1 V s^{-1}, whereas it is not with pristine SWCNT electrodes (fish-like shape of the curve). Reprinted with permission from [206] Copyright (2007) Elsevier Ltd.*

nanotubes [207] but also partly arising from the fact that SWCNTs are one of the few species capable of isolating discrete single molecules containing single isolated spins (e.g. $N@C_{60}$) [208]. Progress in this area is slow but, such materials could one day form the basis of a solid state quantum computer [209].

Acknowledgements

J. S. is indebted to the Royal Society for the previous award of a University Research Fellowship and also to the Warwick Centre for Analytical Science (EPSRC funded Grant EP/F034210/1). M.M. is indebted to NATO, Imra-Europe, Toyota Motor-Corporation, the "Hierarchised Nanomaterials" CNRS program, and the "ACI Nanoscience" government program for their financial support.

References

[1] H. Kataura, Y. Maniwa, M. Abe, A. Fujiwara, T. Kodama, K. Kikuchi, H. Imahori, Y. Misaki, S. Suzuki and Y. Achiba, Optical properties of fullerene and non-fullerene peapods, *Appl. Phys. A*, **74**, 349–354 (2002).

[2] D.A. Morgan, J. Sloan and M.L.H. Green, Direct imaging of *o*-carborane molecules within single walled carbon nanotubes, *Chem. Commun*., 2442–2443 (2002).

[3] M. Koshino, T. Tanaka, N. Solin, K. Suenaga, H. Isobe and E. Nakamura, Imaging of single organic molecules in motion, *Science*, **316**, 853–855 (2007).

[4] L. Guan, Z. Shi, M. Li and Z. Gu, Ferrocene filled single walled carbon nanotubes, *Carbon*, **43**, 2780–2785 (2005).
[5] L.-J. Li, A.N. Khlobystov, J.G. Wiltshire, G.A.D. Briggs and R.J. Nicholas, Diameter-selective encapsulation of metallocenes in single-walled carbon nanotubes, *Nature Mater*., **4**, 481–485 (2005).
[6] A.N. Khlobystov, D.A. Britz and G.A.D. Briggs, Molecules in carbon nanotubes, *Accts. Chem. Res*., **38**, 901–909 (2005).
[7] K. Yanagi, K. Iakoubovskii, H. Matsui, H. Matsuzaki, H. Okamoto, Y. Miyata, Y. Maniwa, S. Kazaoui, N. Minami and H. Kataura, Photosensitive function of encapsulated dye in carbon nanotubes, *J. Am. Chem. Soc*., **129**, 4992–4997 (2007).
[8] X. Fan, E.C. Dickey, P.C. Eklund, K.A. Williams, L. Grigorian, R. Buczko, S.T. Pantelides and S.J. Pennycook, Reversible intercalation of charged iodine chains into carbon nanotubes, *Phys. Rev. Lett*., **84**, 4621–4624 (2000).
[9] L. Guan, K. Suenaga, S. Zujin, Z. Gu and S. Iijima, Polymorphic structures of iodine and their phase transition in confined nanospace, *Nano Lett*., **7**, 1532–1535 (2007).
[10] J. Sloan, J. Hammer, M. Zwiefka-Sibley and M.L.H. Green, The opening and filling of single walled carbon nanotubes (SWTs), *Chem. Commun*., 347–348 (1998).
[11] C.H. Kiang, J.-S. Choi, T.T. Tran and A.D. Bacher, Molecular nanowires of 1 nm diameter from capillary filling of single-walled carbon nanotubes, *J. Phys. Chem. B*, **103**, 7449–7451 (1999).
[12] Y.F. Li, R. Hatakeyama, T. Kaneko, T. Izumida, T. Okada and T. Kato, Electrical properties of ferromagnetic semiconducting single-walled carbon nanotubes, *Appl. Phys. Lett*., **89**, 083117/1–2 (2006).
[13] M. Monthioux, J.-P. Cleuziou and E. Flahaut, Hybrid carbon nanotubes: Strategy, progress, and perspectives, *J. Mater. Res*., **21**, 2774–2793 (2006).
[14] J. Chancolon, F. Archaimbault, S. Bonnamy, A. Traverse, L. Olivi and G. Vlaic, Confinement of selenium inside carbon nanotubes. Structural characterization by X-ray diffraction and X-ray absorption spectroscopy, *J. Non-Cryst. Sol*., **352**, 99–108 (2006).
[15] J.-P. Cleuziou, W. Wernsdorfer, T. Ondarçuhu and M. Monthioux, Magneto-transport in carbon nanotube-templated 1D cobalt-crystal, *Proc. The World Conference on Carbon "CARBON'10"*, July 11–16, Clemson, South Carolina, USA, Extend. Abstr. #626 (CD-Rom) (2010).
[16] P.M. Ajayan and S. Iijima, Capillarity-induced filling of carbon nanotubes, *Nature*, **361**, 333–334 (1993).
[17] P.M. Ajayan, O. Stephan, P. Redlich and C. Colliex, Carbon nanotubes as removable templates for metal oxide nanocomposites and nanostructures, *Nature*, **375**, 564–567 (1995).
[18] J. Mittal, M. Monthioux, H. Allouche and O. Stephan, Room temperature filling of single-wall carbon nanotubes with chromium oxide in open air. *Chem. Phys. Lett*., **339**, 311–318 (2001).
[19] S. Seraphin, D. Zhou, J. Jiao, J.C. Withers and R. Loufty, Yttrium carbide in nanotubes, *Nature,* **362**, 503 (1993).
[20] C. Guerret-Piécourt, Y. Le Bouar, A. Loiseau and H. Pascard, Relation between metal electronic structure and morphology of metal compounds inside carbon nanotubes, *Nature*, **372**, 761–765 (1994).
[21] M. Liu and J.M. Cowley, Encapsulation of lanthanum carbide in carbon nanotubes and carbon nanoparticles, *Carbon*, **33**, 225–232 (1995).
[22] J. Sloan, M.C. Novotny, S.R. Bailey, G. Brown, C. Xu, V.C. Williams, S. Friedrichs, E. Flahaut, R.L. Callendar, A.P.E. York, K.S. Coleman, M L.H. Green, R.E. Dunin-Borkowski and J.L. Hutchison, Two layer 4:4 coordinated KI crystals grown within single walled carbon nanotubes, *Chem. Phys. Lett*., **29**, 61–65 (2000).
[23] R.R. Meyer, J. Sloan, A.I. Kirkland, R.E. Dunin-Borkowski, M.C. Novotny, S.R. Bailey, J.L. Hutchison and M.L.H. Green, Discrete atom imaging of one-dimensional crystals formed within single-walled carbon nanotubes, *Science*, **289**, 1324–1326 (2000).
[24] C. Xu, J. Sloan, G. Brown, S.R. Bailey, V.C. Williams, S. Friedrichs, K.S. Coleman, J.L. Hutchison, R.E. Dunin-Borkowski and M.L.H. Green, 1D lanthanide halide crystals inserted into single-walled carbon nanotubes, *Chem. Commun*., 2427–2428 (2000).
[25] B.C. Satishkumar, A. Taubert and D.E. Luzzi, Filling single wall carbon nanotubes with d- and f-metal chloride and metal nanowires, *J. Nanosci. Nanotech*., **3**, 159–163 (2003).

[26] E. Philp, J. Sloan, A.I. Kirkland, R.R. Meyer, S. Friedrichs, J.L. Hutchison, and M.L.H. Green, An encapsulated helical one dimensional cobalt iodide nanostructure, *Nature Mater.*, **2**, 788–791 (2003).
[27] R. Carter, J. Sloan, A. Vlandas, M.LH. Green, A.I. Kirkland, R.R. Meyer, J.L. Hutchison, P.J.D. Lindan, G. Lin and J. Harding, Correlation of structural and electronic properties in a new low dimensional form of mercury telluride, *Phys. Rev. Lett.*, **96**, 215501.1–215501.4 (2006).
[28] E. Flahaut, J. Sloan, S. Friedrichs, A.I. Kirkland, K.S. Coleman, V.C. Williams, N. Hanson, J.L. Hutchison and M.L.H. Green, Crystallisation of 2H and 4H PbI_2 in carbon nanotubes of varying diameters and morphologies, *Chem. Mater.*, **18**, 2059–2069 (2006).
[29] W.K. Hsu, S. Trasobares, H. Terrones, M. Terrones, N. Grobert, Y.Q. Zhu, W.Z. Li, J.P. Hare, R. Escudero, H.W. Kroto and D.R.M. Walton, Electrolytic formation of carbon-sheathed mixed Sn-Pb nanowires, *Chem. Mater.*, **11**, 1747–1751 (1998).
[30] N. Grobert, M. Mayne, R.R.M. Walton, H.W. Kroto, M. Terrones, R. Kamalakaran, T. Seeger, M. Ruhle, H. Terrones, J. Sloan, R.E. Dunin-Borkowski and J.L. Hutchison, Alloy nanowires: Invar inside carbon nanotubes, *Chem. Commun.*, 471–472 (2001).
[31] J.Q. Hu, Y. Bando, J.H. Zhan, C.Z. Li and D. Golberg, Mg_3N_2-Ga: Nanoscale semiconductor-liquid metal heterojunctions inside graphitic carbon nanotubes, *Adv. Mater.*, **19**, 1342–1346 (2007).
[32] S.B. Fagan, A.G. Souza Filho, P. Corio, J. Mendes Filho and M.S. Dresselhaus, Electronic properties of Ag- and CrO_3-filled carbon nanotubes, *Chem. Phys. Lett.*, **406**, 54–59 (2005).
[33] J.A. Alonso, J.S. Arellano, L.M. Molina, A. Rubio and M.J. Lopez, Interaction of molecular and atomic hydrogen with single-wall carbon nanotubes, *IEEE Trans. Nanotech.*, **3**, 304–310 (2004).
[34] K. Koga, G.T. Gao, H. Tanaka and X.C. Zeng, Formation of ordered ice nanotubes inside carbon nanotubes, *Nature*, **412**, 802–805 (2001).
[35] Y. Maniwa, M. Abe, H. Kataura, S. Suzuki, Y. Achiba, H. Kira and K. Matsuda, Phase transition in confined water inside carbon nanotubes, *J. Phys. Soc. Jpn.*, **71**, 2863–2866 (2002).
[36] M.S. Dresselhaus, G. Dresselhaus and R. Saito, Physics of carbon nanotubes, *Carbon*, **33**, 883–891 (1995).
[37] J. Sloan, A.I. Kirkland, J.L. Hutchison and M.L.H. Green, Integral atomic layer architectures of 1D crystals inserted into single walled carbon nanotubes, *Chem. Commun.*, 1319–1332 (2002).
[38] D. Ugarte, A. Chatelain and W.A. de Heer, Nanocapillarity and chemistry in carbon nanotubes, *Science*, **274**, 1897–1899 (1996).
[39] E. Dujardin, T.W. Ebbesen, A. Krishnan and M.M.J. Treacy, Wetting of single shell carbon nanotubes, *Adv. Mater.*, **10**, 1472–1475 (1998).
[40] E. Dujardin, T.W. Ebbesen, H. Hiura and K. Taginaki, Capillarity and wetting of carbon nanotubes, *Science*, **265**, 1850–1852 (1994).
[41] P.M. Ajayan, T.W. Ebbesen, T. Ichihashi, S. Iijima, K. Tanigaki and H. Hiura, Opening carbon nanotubes with oxygen and implications for filling, *Nature*, **362**, 522–525 (1993).
[42] Y. Saito and T. Yoshikawa, Bamboo-shaped carbon tube filled partially with nickel, *J. Cryst. Growth*, **134**, 154–156 (1993).
[43] S. Iijima, Helical microtubules of graphite carbon, *Nature*, **354**, 56–58 (1991).
[44] S. Iijima and T. Ichihashi, Single-shell carbon nanotubes of 1–nm diameter. *Nature*, **363**, 603–605 (1993).
[45] D.S. Bethune, C.H. Kiang, M.S. De Vries, G. Gorman, R. Savoy, J. Vasquez and R. Breyers, Cobalt catalysed growth of carbon nanotubes with single-atomic-layer walls, *Nature*, **363**, 605–607 (1993).
[46] B.W. Smith, M. Monthioux and D.E. Luzzi, Encapsulated C_{60} in carbon nanotubes, *Nature*, **396**, 323–324 (1998).
[47] B. Burteaux, A. Claye, B.W. Smith, M. Monthioux, D.E. Luzzi and J.E. Fischer, Abundance of encapsulated C_{60} in single-wall carbon nanotubes, *Chem. Phys. Lett.*, **310**, 21–24 (1999).
[48] J.S. Bendall, A. Ilie, M.E. Welland, J. Sloan and M.L.H. Green, Thermal stability and reactivity of metal halide filled single walled carbon nanotubes, *J. Phys. Chem.*, **110**, 6569–6573 (2006).
[49] J. Sloan, J. Cook, M.L.H. Green, J.L. Hutchison and R. Tenne, Crystallization inside fullerene-related structures, *J. Mater. Chem.*, **7**, 1089–1095 (1997).
[50] D. Ugarte, T. Stöckli, J.M. Bonard, A. Châtelain and W.A. de Heer, Filling carbon nanotubes. *Appl. Phys. A*, **67**, 101–105 (1998).

[51] A. Loiseau and H. Pascard, Synthesis of long carbon nanotubes filled with Se, S, Sb, and Ge by the arc method, *Chem. Phys. Lett.*, **256**, 246 (1996).
[52] P.C.P. Watts, W.K. Hsu, V. Kotzeva and G.Z. Chen, Fe-filled carbon nanotube-polystyrene: RCL composites, *Chem. Phys. Lett*., **366**, 42–50 (2002).
[53] J.Y. Dai, J.M. Lauerhaas, A.A. Setlur and R.P.H. Chang, Synthesis of carbon-encapsulated nanowires using polycyclic aromatic hydrocarbon precursors, *Chem. Phys. Lett*., **258**, 547–553 (1996).
[54] C.N.R. Rao, R. Sen, B.C. Satishkumar and A. Govindaraj, Large aligned-nanotube bundles from ferrocene pyrolysis, *Chem. Commun*., 1525–1526 (1998).
[55] A. Leonhardt, M. Ritschel, R. Kozhuharova, A. Graff, T. Mühl, R. Huhle, I. Mönch, D. Elefant and C.M. Schneider, Synthesis and properties of filled carbon nanotubes, *Diamond Relat. Mater*., **12**, 790–793 (2003).
[56] N. Demoncy, O. Stéphan, N. Brun, C. Colliex, A. Loiseau and H. Pascard, Filling carbon nanotubes with metals by the arc discharge method: The key role of sulphur, *Eur. Phys. J. B*, **4**, 147–157 (1998).
[57] A. Loiseau and F. Willaime, Filled and mixed nanotubes: From TEM studies to the growth mechanism within a phase-diagram approach, *Appl. Surf. Sci*., **164**, 227–240 (2000).
[58] Y. Zhang, S. Iijima, Z. Shi and Z. Gu, Defects in arc-discharge produced single-walled carbon nanotubes, *Philos. Mag. Lett*., **79**, 473–479 (1999).
[59] J. Sloan, R.E. Dunin-Borkowski, J.L. Hutchison, K.S. Coleman, V.C. Williams, J.B. Claridge, A.P.E. York, C. Xu, S.R. Bailey, G. Brown, S. Friedrichs and M.L.H. Green, The size distribution, imaging and obstructing properties of C_{60} and higher fullerenes formed within arc-grown single walled carbon nanotubes, *Chem. Phys. Lett*., **316**, 191–198 (2000).
[60] S.C. Tsang, Y.K. Chen, P.J.F. Harris and M.L.H. Green, A simple chemical method of opening and filling carbon nanotubes, *Nature*, **372**, 159–162 (1994).
[61] B.C. Satishkumar, A. Govindaraj, J. Mofokeng, G.N. Subbanna and C.N.R. Rao, Novel experiments with carbon nanotubes: Opening, filling, closing, and functionalizing nanotubes, *J. Phys. B*, **29**, 4925–4934 (1996).
[62] M. Monthioux, Filling single wall carbon nanotubes, *Carbon*, **40**, 1809–1823 (2002).
[63] S. Berber, Y.-K. Kwon and D. Tománek, Microscopic formation mechanism of nanotube peapods, *Phys. Rev. Lett*., **88**, 185502/1–4 (2002).
[64] B.W. Smith and D.E. Luzzi, Formation mechanism of fullerene peapods and coaxial tubes: A path to large scale synthesis, *Chem. Phys. Lett*., **321**, 169–174 (2000).
[65] G. Brown, S. Bailey, J. Sloan, C. Xu, S. Friedrichs, E. Flahaut, K.S. Coleman, J.L. Hutchison, R.E. Dunin-Borkowski and M.L.H. Green, Electron beam induced in situ clusterization of 1D $ZrCl_4$ chains within single-walled carbon nanotubes, *Chem. Commun*., 845–846 (2001).
[66] J. Chancolon, F. Archaimbault, A. Pineau and S. Bonnamy, Filling of carbon nanotubes with selenium by vapor phase process, *J. Nanosci. Nanotechnol*., **6**, 1–5 (2006).
[67] P.M.F.J. Costa, J. Sloan, T. Rutherford and M.L.H. Green, Encapsulation of Re_xO_y clusters within single-walled carbon nanotubes and their *in tubulo* reduction and sintering to Re metal, *Chem. Mater*., **17**, 6579–6582 (2005).
[68] W. Mickelson, S. Aloni, W.-Q. Han, J. Cumings and A. Zettl, Packing C_{60} in boron nitride nanotubes, *Science*, **300**, 467–469 (2003).
[69] T. Fröhlich, P. Scharff, W. Schliefke, H. Romanus, V. Gupta, C. Siegmund, O. Ambacher and L. Spiess, Insertion of C_{60} into multi-wall carbon nanotubes: A synthesis of C_{60}@MWCNT, *Carbon*, **42**, 2759–2762 (2004).
[70] B.M. Kim, S. Qian and H.H. Bau, Filling carbon nanotubes with particles, *Nano Lett.*, **5**, 873–878 (2005).
[71] G. Korneva, H. Ye, Y. Gogotsi, D. Halverson, G. Friedman, J.-C. Bradley and K.G. Kornev, Carbon nanotubes loaded with magnetic nanoparticles, *Nano Lett*., **5**, 879–884 (2005).
[72] S. Iijima, M. Yudasaka, R. Yamada, S. Bandow, K. Suenaga, F. Kokai and K. Takahashi, Nano-aggregates of single-walled graphitic carbon nano-horns, *Chem. Phys. Lett*., **309**, 165–170 (1999).
[73] A. Hashimoto, H. Yorimitsu, K. Ajima, K. Suenaga, H. Isobe, J. Miyawaki, M. Yudasaka, S. Iijima and E. Nakamura, Selective deposition of a gadolinium (III) cluster in a hole opening of single-wall carbon nanohorn, *Proc. Natl. Acad. Sci*., **101**, 8527–8530 (2004).

[74] Z.L. Zhang, B. Li, Z.J. Shi, Z.N. Gu, Z.Q. Xue and L.M. Peng, Filling of single-walled carbon nanotubes with silver, *J. Mater. Res*., **15**, 2658–2661 (2000).
[75] A. Govindaraj, B.C. Satishkumar, M. Nath and C.N.R. Rao, Metal nanowires and intercalated metal layers in single-walled carbon nanotube bundles, *Chem. Mater*., **12**, 202–204 (2000).
[76] Z. Liu, M. Koshino, K. Suenaga, A. Mrzel, H. Kataura and S. Iijima, Transmission electron microscopy imaging of individual functional groups of fullerene derivatives, *Phys. Rev. Lett*., **96**, 088304/1–4 (2006).
[77] Z. Liu, K. Yanagi, K. Suenaga, H. Kataura and S. Iijima, Imaging the dynamic behaviour of individual retinal chromophores confined inside carbon nanotubes, *Nature Nanotechnol*., **2**, 422–425 (2007).
[78] F. Simon, H. Kuzmany, H. Rauf, T. Pichler, J. Bernardi, H. Peterlik, L. Korecz, F. Fülöp and A. Jànossy, Low temperature fullerene encapsulation in single wall carbon nanotubes: Synthesis of $N@C_{60}$@SWCNT, *Chem. Phys. Lett*., **383**, 362–367 (2004).
[79] D.A. Britz, A.N. Khlobystov, J. Wang, A.S. O'Neil, M. Poliakoff, A. Ardavan and G.A.D. Briggs, Selective host-guest interaction of single-walled carbon nanotubes with functionalized fullerenes, *Chem. Commun*., 176–177 (2004).
[80] D.A. Britz, A.N. Khlobystov, K. Porfyrakis, A. Ardavan and G.A.D. Briggs, Filling of fullerene oxide in supercritical CO_2, *Chem. Commun*., 37–38 (2005).
[81] J. Mittal, H. Konno and M. Inagaki, Synthesis of GICs of Cr^{VI} compound using CrO_3 and HCl at room temperature, *Synth. Met*., **96**, 103–108 (1998).
[82] G. Brown, S.R. Bailey, M. Novotny, R. Carter, E. Flahaut, K.S. Coleman, J.L. Hutchison, M.L.H. Green and J. Sloan, High-yield incorporation and washing properties of halides incorporated into single walled carbon nanotubes, *Appl. Phys. A*, **76**, 1–6 (2003).
[83] B.C. Satishkumar, A. Taubert and D.E. Luzzi, Filling single wall carbon nanotubes with d- and f-metal chloride and metal nanowires, *J. Nanosci. Nanotechnol*., **3**, 159–163 (2003).
[84] M. Hulman, H. Kuzmany, P.M.F.J. Costa, S. Friedrichs and M.L.H. Green, Light-induced instability of PbO-filled single wall carbon nanotubes, *Appl. Phys. Lett*., **85**, 2068–2070 (2004).
[85] J. Sloan, D.M. Wright, H.G. Woo, S. Bailey, G. Brown, A.P.E. York, K.S. Coleman, J.L. Hutchison and M.L.H. Green, Capillarity and silver nanowire formation observed in single walled carbon nanotubes, *Chem. Commun*., 699–700 (1999).
[86] L. Grigorian, K.A. Williams, S. Fang, G.U. Sumanasekera, A.L. Loper, E.C. Dickey, S.J. Pennycook and P.C. Eklund, Reversible intercalation of charged iodine chains into carbon nanotube ropes, *Phys. Rev. Lett*., **80**, 5560–5563 (1998).
[87] X. Fan, E.C. Dickey, P.C. Eklund, K.A. Williams, L. Grigorian, R. Buczko, S.T. Pantelides and S.J. Pennycook, Atomic arrangement of iodine atoms inside single-walled carbon nanotubes, *Phys. Rev. Lett*., **84**, 4621–4624 (2000).
[88] J. Mittal, M. Monthioux and H. Allouche, Synthesis of SWNT based hybrid nanomaterials from photolysis-enhanced chemical processes, in *Proc. 25th Biennial Conference on Carbon*, Lexington, KY, USA, Novel/14.2 (2001).
[89] J. Mittal, M. Monthioux, V. Serin and J.-P. Cleuziou, UV photolysis: An alternative for the synthesis of hybrid carbon nanotubes, in *Chinese-French Workshop on Carbon Materials*, September 30-October 1, Orléans, France (2005).
[90] G.-H. Jeong, R. Hatakeyama, T. Hirata, K. Tohji, K. Motomiya, N. Sato and Y. Kawazoe, Structural deformation of single walled carbon nanotubes and fullerene encapsulation due to magnetized-plasma ion irradiation, *Appl. Phys. Lett*., **79**, 4213–4215 (2001).
[91] G-H. Jeong, R. Hatakeyama, T. Hirata, K. Tohji, K. Motomiya, T. Yaguchi and Y. Kawazoe, Formation and structural observation of cesium encapsulated in single-walled carbon nanotubes, *Chem. Commun.*, 152–153 (2003).
[92] B.-Y. Sun, Y. Sato, K. Suenaga, T. Okazaki, N. Kishi, T. Sugai, S. Bandow, S. Iijima and H. Shinohara, Entrapping of exohedral metallofullerenes in carbon nanotubes: $(CsC_{60})_n$@ SWNT nanopeapods, *J. Am. Chem. Soc*., **127**, 17972–17973 (2005).
[93] T. Pichler, A. Kukovecz, H. Kuzmany, H. Kataura and Y. Achiba, Quasicontinuous electron and hole doping of C_{60} peapods, *Phys. Rev. B*, **67**, 125416.1–125416.7 (2003).
[94] M. Kalbac, L. Kavan, M. Zukalova and L. Dunsch, Two positions of potassium in chemically doped C_{60} peapods: an in situ spectroelectrochemical study, *J. Phys. Chem. B*, **108**, 6275–6280 (2004).

[95] T. Shimada, Y. Ohno, T. Okazaki, T. Sugai, K. Suenaga, S. Kishimoto, T. Mizutani, T. Inoue, R. Taniguchi, N. Fukui, H. Okubo and H. Shinohara, Transport properties of C_{78}, C_{90} and Dy@C_{82} fullerenes-nanopeapods by field effect transistors, *Physica E*, **21**, 1089–1092 (2004).

[96] D.E. Luzzi, B.W. Smith, R. Russo, B.C. Satishkumar, F. Stercel and N. Nemes, Encapsulation of metallofullerenes and metallocenes in carbon nanotubes, in *Electronic Properties of Molecular Nanostructures*, H. Kuzmany, J. Fink, M. Mehring and S. Roth (eds.), American Institute of Physics Conference Proceedings Series, **591**, 622–626 (2001).

[97] H. Shiozawa, H. Rauf, T. Pichler, M. Knupfer, M. Kalbac, S. Yang, L. Dunsch, B. Büchner, D. Batchelor and H. Kataura, Effective valency of Dy ions in $Dy_3N@C_{80}$ metallofullerenes in peapods, in *Electronic Properties of Molecular Nanostructures*, H. Kuzmany, J. Fink, M. Mehring and S. Roth (eds.), American Institute of Physics Conference Proceedings Series, **786**, 325–328 (2002).

[98] K. Suenaga, M. Tence, C. Mory, C. Colliex, H. Kato, T. Okazaki, H. Shinohara, K. Hirahara, S. Bandow and S. Iijima, Element selective single atom imaging, *Science*, **290**, 2280–2282 (2000).

[99] K. Suenaga, K. Hirahara, S. Bandow, S. Iijima, T. Okazaki, H. Kato and H. Shinohara, Core level spectroscopy on the valence state of encaged metal in metallofullerenes-peapods, in *Electronic Properties of Molecular Nanostructures*, H. Kuzmany, J. Fink, M. Mehring and S. Roth (eds.), American Institute of Physics Conference Proceedings Series, **591**, 256–260 (2001).

[100] P.W. Chiu, G. Gu, G.T. Kim, G. Philipp, S. Roth, S.F. Yang and S. Yang, Temperature-induced change from *p* to *n* conduction in metallofullerene nanotube peapods, *Appl. Phys. Lett*., **79**, 3845–3847 (2001).

[101] T. Okazaki, K. Suenaga, K. Hirahara, S. Bandow, S. Iijima and H. Shinohara, Real time reaction dynamics in carbon nanotubes, *J. Amer. Chem. Soc*., **123**, 9673–9674 (2001).

[102] T. Okazaki, K. Suenaga, K. Hirahara, S. Bandow, S. Iijima and H. Shinohara, Electronic and geometric structures of metallofullerenes peapods, *Physica B*, **323**, 97–99 (2002).

[103] K. Suenaga, T. Okazaki, C.-R. Wang, S. Bandow, H. Shinohara and S. Iijima, Direct imaging of $Sc_2@C_{84}$ molecules encapsulated inside single-wall carbon nanotubes by high resolution electron microscopy with atomic sensitivity, *Phys. Rev. Lett*., **90**, 055506/1–4 (2003).

[104] K. Suenaga, R. Taniguchi, T. Shimada, T. Okazaki, H. Shinohara and S. Iijima, Evidence for the intramolecular motion of Gd atoms in a $Gd_2@C_{92}$ nanopeapod, *Nano Lett*., **3**, 1395–1398 (2003).

[105] D.M. Guldi, M. Marcaccio, D. Paolucci, F. Paolucci, N. Tagmatarchis, D. Tasis, E. Vasquez and M. Prato, Single wall carbon nanotube-ferrocene nanohybrids: Observing intramolecular electron transfer in functionalized SWNTs, *Angew. Chem. Int. Ed*., **42**, 4206–4209 (2003).

[106] H. Qiu, Z. Shi, Z. Gu and J. Qiu, Controllable preparation of triple-walled carbon nanotubes and their growth mechanism, *Chem. Commun*., 1092–1094 (2007).

[107] L. Guan, K. Suenaga and S. Iijima, Smallest carbon nanotube assigned with atomic resolution accuracy, *Nano Lett*., **8**, 459–462 (2008).

[108] H. Shiozawa, T. Pichler, A. Grüneis, R. Pfeiffer, H. Kuzmany, Z. Liu, K. Suenaga and H.Kataura, A Catalytic reaction inside a single-walled carbon nanotube, *Adv. Mater*. **20**, 1443–1449 (2008).

[109] T. Takenobu, T. Takano, M. Shiraishi, Y. Murakami, M. Ata, H. Kataura, Y. Achiba and Y. Iwasa, Stable and controlled amphoteric doping by encapsulation of organic molecules inside carbon nanotubes, *Nature Mater*., **2**, 683–688 (2003).

[110] H. Kataura, Y. Maniwa, T. Kodama, K. Kikuchi, S. Susuki, Y. Achiba, K. Sugiura, S. Okubo and K. Tsukagoshi, One dimensional system in carbon nanotubes, in *Electronic Properties of Molecular Nanostructures*, H. Kuzmany, J. Fink, M. Mehring and S. Roth (eds.), American Institute of Physics Conference Proceedings, **685**, 349–353 (2003).

[111] D.M. Kammen, T.E. Lipman, A.B. Lovins, P.A. Lehman, J.M. Eiler, T.K. Tromp, R.-L. Shia, M. Allen and Y.L. Yung, Assessing the future hydrogen economy, *Science*, **302**, 226–229 (2003).

[112] A. Kuznetsova, J.T. Yates Jr., J. Li and R.E. Smalley, Physical adsorption of xenon in open single walled carbon nanotubes: Observation of a quasi-one-dimensional confined Xe phase, *J. Chem. Phys*., **112**, 9590–9598 (2000).

[113] A. Fujiwara, K. Ishii, H. Suematsu, H. Kataura, Y. Maniwa, S. Susuki and Y. Achiba, Gas adsorption in the inside and outside of single-walled carbon nanotubes, *Chem. Phys. Lett*., **336**, 205–211 (2001).

[114] K.A. Williams and P.C. Eklund, Monte Carlo simulations of H_2 physisorption in finite-diameter carbon nanotube ropes, *Chem. Phys. Lett*., **320**, 352–358 (2000).

[115] A.C. Dillon, K.M. Jones, T.A. Bekkedahl, C.H. Kiang, D.S. Bethune and M. J. Heben, Storage of hydrogen in single walled carbon nanotubes, *Nature*, **386**, 377–379 (1997).

[116] M. Hirscher, M. Becher, M. Haluska, U. Dettlaff-Weglikowska, A. Quintel, G.S. Duesberg, Y.M. Choi, P. Downes, M. Hulman, S. Roth, I. Stepanek and P. Bernier, Hydrogen storage in sonicated carbon materials, *Appl. Phys. Mater. Sci. Process*, **2**, 129–132 (2001).

[117] S. Farhat, B. Weinberger, F.D. Lamari, T. Izouyar, L. Noé and M. Monthioux, Performance of carbon arc-discharge nanotubes to hydrogen energy storage, *J. Nanosci. Nanotechnol*., **7**, 3537–3542 (2007).

[118] J. Sloan, G. Matthewman, C. Dyer-Smith, A.-Y. Sung, Z. Liu, K. Suenaga, A.I. Kirkland and E. Flahaut, Direct imaging of the structure, relaxation and sterically constrained motion of encapsulated tungsten polyoxometalate Lindqvist ions within carbon nanotubes, *ACS Nano*, **2**, 966–976 (2008).

[119] P. Corio, A.P. Santos, P.S. Santos, M.L.A. Temperini, V.W. Brar, M.A. Pimenta and M. S. Dresselhaus, Characterization of single wall carbon nanotubes filled with silver and with chromium compounds, *Chem. Phys. Lett*., **383**, 475–480 (2004).

[120] E. Borowiak-Palen, M.H. Rummeli, E. Mendoza, S.J. Henley, D.C. Cox, C.H.P. Poa, V. Stolojan, T. Gemming, T. Pichler and S.R.P. Silva, Silver intercalated carbon nanotubes, in *Electronic Properties of Molecular Nanostructures*, H. Kuzmany, J. Fink, M. Mehring and S. Roth (eds.), American Institute of Physics Proceedings Series, **786**, 236–239 (2005).

[121] E. Borowiak-Palen, E. Mendoza, A. Bachmatiuk, M.H. Rummeli, T. Gemming, J. Nogues, V. Skumryev, R.J. Kalenczuk, T. Pichler and S.R.P. Silva, Iron filled single-wall carbon nanotubes: A novel ferromagnetic medium, *Chem. Phys. Lett*., **421**, 129–133 (2006).

[122] J. Jorge, E. Flahaut, F. Gonzalez-Jimenez, G. Gonzalez, J. Gonzalez, E. Belandria, J.-M. Broto and B. Raquet, Preparation and characterization of α-Fe nanowires located inside double wall carbon nanotubes, *Chem. Phys. Lett*., **457**, 347–351 (2008).

[123] J. Sloan, A.I. Kirkland, J.L. Hutchison and M.L.H. Green, Aspects of crystal growth within carbon nanotubes, *C. R. Phys*., **4**, 1063–1074 (2003).

[124] J. Sloan, S. Friedrichs, R.R. Meyer, A.I. Kirkland, J.L. Hutchison and M.L.H. Green: Structural changes induced in nanocrystals of binary compounds confined within single walled carbon nanotubes: A brief review, *Inorg. Chim. Acta*, **330**, 1–12 (2002).

[125] J. Sloan and M.L.H. Green, Synthesis and characterisation of materials incorporated within carbon nanotubes, in *Fullerenes: Chemistry, Physics and Technology*, K.M. Kadish and R.S. Ruoff (eds.), John Wiley & Sons, Inc., New York, 826–828 (2000).

[126] L.-J. Li, T.-W. Lin, J. Doig, I.B. Mortimer, J.G. Wiltshire, R.A. Taylor, J. Sloan, M.L.H. Green and R.J. Nicholas, Crystal-encapsulation-induced band-structure change in single-walled carbon nanotubes: Photoluminescence and Raman spectra, *Phys. Rev. B*, **74**, 245418/1–5 (2006).

[127] E. Flahaut, J. Sloan, K.S. Coleman and M.L.H. Green, Synthesis of 1D p-block halide crystals within single walled carbon nanotubes, in *Electronic Properties of Molecular Nanostructures*, H. Kuzmany, J. Fink, M. Mehring and S. Roth (eds), American Institute of Physics Proceedings Series, **591**, 283–286 (2001).

[128] G. Chen, J. Qiu and H. Qiu, Filling double-walled carbon nanotubes with AgCl nanowires, *Scripta Mater*., **58**, 457–460 (2008).

[129] J. Sloan, S. Friedrichs, E. Flahaut, G. Brown, S.R. Bailey, K.S. Coleman, C. Xu, M.L.H. Green, J.L. Hutchison, A.I. Kirkland and R.R. Meyer, The characterization of subnanometer scale structures within single walled carbon nanotubes, in *Electronic Properties of Molecular Nanostructures*, H. Kuzmany, J. Fink, M. Mehring and S. Roth (eds.), American Institute of Physics Proceedings Series, **591**, 277–282 (2001).

[130] J. Sloan, M. Terrones, S. Nufer, S. Friedrichs, S.R. Bailey, H.G. Woo, M. Rühle, J.L. Hutchison and M.L.H. Green, Metastable one-dimensional $AgCl_{1-x}I_x$ solid-solution wurzite 'tunnel' crystals formed within single walled carbon nanotubes, *J. Am. Chem. Soc*., **124**, 2116–2117 (2002).

[131] J. Sloan, M. Terrones, S. Nufer, S. Friedrichs, S.R. Bailey, H-G. Woo, M. Rühle, J.L. Hutchison and M.L.H. Green, Spatially resolved EELS applied to the study of a one-dimensional solid solution of $AgCl_{1-x}I_x$ formed within single-wall carbon nanotubes, in *Electronic Properties of Molecular Nanostructures*, H. Kuzmany, J. Fink, M. Mehring and S. Roth (eds.), American Institute of Physics Proceedings Series, **633**, 135–139 (2002).

[132] P.M.F.J. Costa, S. Friedrichs, J. Sloan and M.L.H. Green, Imaging lattice defects and distortions in alkali-metal iodides encapsulated within double-walled carbon nanotubes, *Chem. Mater*. **17**, 3122–3129 (2005).

[133] M.V. Chernysheva, A.A. Eliseev, A.V. Lukashin, Y.D. Tretyakov, S.V. Savilov, N.A. Kiselev, O.M. Zhigalina, A.S. Kumskov, A.V. Krestinin and J.L. Hutchison, Filling of single-walled carbon nanotubes by CuI nanocrystals via capillary technique, *Physica E*, **37**, 62–65 (2007).

[134] J. Sloan, S.J. Grosvenor, S. Friedrichs, A. Kirkland, J.L. Hutchison and M.L.H. Green, A one-dimensional BaI_2 chain with five-and six-coordination, formed within a single-walled carbon nanotube, *Angew. Chem., Int. Ed*., **41**, 1156–1159 (2002).

[135] S. Friedrichs, R.R. Meyer, J. Sloan, A.I. Kirkland, J.L. Hutchison and M.L.H. Green, Complete characterization of a Sb_2O_3/(21,-8)SWNT inclusion composite, *Chem. Commun*., 929–930 (2001).

[136] S. Friedrichs, J. Sloan, M.L.H. Green, J.L. Hutchison, R.R. Meyer and A.I. Kirkland, Simultaneous determination of inclusion crystallography and nanotube conformation for a Sb_2O_3/single-walled nanotube composite. *Phys. Rev. B*, **64**, 045406/1–8 (2001).

[137] N. Thamavaranukup, H.A. Höppe, L. Ruiz-Gonzalez, P.M.F.J. Costa, J. Sloan, A. Kirkland and M.L.H. Green, Single-walled carbon nanotubes filled with *M* OH (*M* = K, Cs) and then washed and refilled with clusters and molecules, *Chem. Commun*., 1686–1697 (2004).

[138] P.G. Gennes, F. Brochard-Wyart and D. Quéré, *Capillarity and Wetting Phenomena: Drops, Bubbles, Pearls, Waves*, Springer, New York (2004).

[139] M. Terrones, N. Grobert, W.K. Hsu, Y.Q. Zhu, W.B. Hu, H. Terrones, J.P. Hare, H.W. Kroto and D.R. Walton, Advances in the creation of filled nanotubes and novel nanowires, *MRS Bull*., **24**, 43–49 (1999).

[140] M.R. Pederson and J.Q. Broughton, Nanocapillarity in fullerene tubules, *Phys. Rev. Lett*., **69**, 2689–2692 (1992).

[141] M. Wilson and P.A. Madden, Growth of ionic crystals in carbon nanotubes, *J. Am. Chem. Soc*., **123**, 2101–2102 (2001).

[142] A.A. Sofronov, V.V. Ivanovskaya, Y.N. Makurin and A.L. Ivanovskii, New one-dimensional crystals of $(Sc,Ti,V)_8C_{12}$ metallocarbohedrenes in carbon and boron–nitrogen (12,0) nanotubes: quantum chemical simulation of the electronic structure, *Chem. Phys. Lett*., **351**, 35–41 (2002).

[143] R.J. Mashl, S. Joseph, N.R. Aluru and E. Jakobsson, Anomalously immobilized water: A new water phase induced by confinement in nanotubes, *Nano Lett*., **3**, 589–592 (2003).

[144] H. Gao, Y. Kong and D. Cui, Spontaneous insertion of DNA oligonucleotides into carbon nanotubes, *Nano Lett*., **3**, 471–473 (2003).

[145] Y. Guo, Y. Kong, W. Guo and H. Gao, Structural transition of copper nanowires confined in single-walled carbon nanotubes, *J. Comput. Theor. Nanosci*., **1**, 93–98 (2004).

[146] G. Kim, Y. Kim and J. Ihm, Encapsulation and polymerization of acetylene molecules inside a carbon nanotube, *Chem. Phys. Lett*., **415**, 279–282 (2005).

[147] J. Zhang, X.Q. Zhang, H. Li and K.M. Liew, The structures and electrical transport properties of germanium nanowires encapsulated in carbon nanotubes, *Appl. Phys*., **102**, 073709/1–5 (2007).

[148] C.-K. Yang, J. Zhao and J.P. Lu, Magnetism of transition-metal/carbon-nanotube hybrid structures, *Phys. Rev. Lett*., **90**, 257203/1–4 (2003).

[149] Y.-J. Kang, J. Choi, C-Y. Moon and K.J. Chang, Electronic and magnetic properties of single-wall carbon nanotubes filled with iron atoms, *Phys. Rev. B*, **71**, 115441.1–115441.7 (2005).

[150] M. Weissmann, G. García, M. Kiwi and R. Ramírez, Theoretical study of carbon-coated iron nanowires, *Phys. Rev. B*, **70**, 201401/1–4 (2004).

[151] M. Weissmann, G. García, M. Kiwi, R. Ramírez and C-C. Fu, Theoretical study of iron-filled carbon nanotubes, *Phys. Rev. B*, **73**, 125435/1–8 (2004).

[152] N. Fujima and T. Oda, Structures and magnetic properties of iron chains encapsulated in tubal carbon nanocapsules, *Phys. Rev. B*, **71**, 115412/1–9 (2005).
[153] B.W. Smith, M. Monthioux and D.E. Luzzi, Carbon nanotube encapsulated fullerenes: A unique class of hybrid materials, *Chem. Phys. Lett*, **315**, 31–36 (1999).
[154] D.E. Luzzi and B.W. Smith, Carbon cage structures in single wall carbon nanotubes: A new class of materials, *Carbon*, **38**, 1751–1756 (2000).
[155] S. Bandow, M. Takizawa, K. Hirahara, M. Yudasaka and S. Iijima, Raman scattering study of double-wall carbon nanotubes derived from the chains of fullerenes in single-wall carbon nanotubes, *Chem. Phys. Lett*., **337**, 48–54 (2001).
[156] Y. Sakurabayashi, M. Monthioux, K. Kishita, Y. Suzuki, T. Kondo and M. Le Lay, Tailoring double wall carbon nanotubes, in *Electronic Properties of Molecular Nanostructures*, H. Kuzmany, J. Fink, M. Mehring and S. Roth (eds.), American Institute of Physics Conference Proceedings, **685**, 302–305 (2003).
[157] C. Arrondo, M. Monthioux, Y. Kishita and M. Le Lay, In situ coalescence of aligned C_{60} in peapods, in *Electronic Properties of Molecular Nanostructures*, H. Kuzmany, J. Fink, M. Mehring and S. Roth (eds.), American Institute of Physics Conference Proceedings, **786**, 329–332 (2005).
[158] C. Kramberger, A. Waske, K. Biedermann, T. Pichler, T. Gemming, B. Büchner and H. Kataura, Tailoring carbon nanostructures via temperature and laser irradiation, *Chem. Phys. Lett.*, **407**, 254–259 (2005).
[159] M. Kalbac, L. Kavan, L. Juha, S. Civis, M. Zukalova, M. Bittner, P. Kubat, V. Vorlicek and L. Dunsch, Transformation of fullerene peapods to double-walled carbon nanotubes induced by UV radiation, *Carbon*, **43**, 1610–1616 (2005).
[160] M. Yoon, S. Berber and D. Tománek, Energetics and packing of fullerenes in nanotube peapods, *Phys. Rev. B*, **71**, 155406/1–4 (2005).
[161] A.F. Wells, in *Structural Inorganic Chemistry*, Oxford University Press, Oxford (1990).
[162] R. Kreizman, S.-Y. Hong, J. Sloan, R. Popovitz-Biro, A. Albu-Yaron, G. Belén Ballesteros, B.G. Davis, M.L.H. Green and R. Tenne, Core-shell PbI_2@WS_2 inorganic nanotubes from capillary wetting, *Angew. Chem., Int. Ed*., **48**, 1230–1233 (2009).
[163] M. Wilson, Structure and phase stability of novel 'twisted' crystal structures in carbon nanotubes, *Chem. Phys. Lett*., **366**, 504–509 (2002).
[164] M. Wilson, The formation of low-dimensional chiral inorganic nanotubes by filling single-walled carbon nanotubes, *Chem. Phys. Lett*., **397**, 340–343 (2004).
[165] J. Vavro, M.C. Llaguno, B.C. Satishkumar, D.E. Luzzi and J.E. Fischer, Electrical and thermal properties of C_{60}-filled single-wall carb on nanotubes, *Appl. Phys. Lett*., **80**, 1450–1452 (2002).
[166] K. Hirahara, K. Suenaga, S. Bandow, H. Kato, T. Okazaki, H. Shinohara and S. Iijima, One-dimensional metallofullerene crystal generated inside single-walled carbon nanotubes, *Phys. Rev. Lett*., **85**, 5384–5387 (2000).
[167] H. Hongo, F. Nihey, M. Yudasaka, T. Ichihashi and S. Iijima, Transport properties of single-wall carbon nanotubes with encapsulated C_{60}, *Physica B*, **323**, 244–245 (2002).
[168] P.W. Chiu, S.F. Yang, S.H. Yang, G. Gu and S. Roth, Temperature dependence of conductance character in nanotube peapods, *Appl. Phys. A*, **76**, 463–467 (2003).
[169] Y. Cho, S. Han, G. Kim, H. Lee and J. Ihm, Orbital hybridization and charge transfer in carbon nanopeapods, *Phys. Rev. Lett*., **90**, 106402/1–4 (2003).
[170] A. Rochefort, Electronic and transport properties of carbon nanotube peapods, *Phys. Rev. B*, **67**, 115401/1–3 (2003).
[171] P. Utko, J. Nygard, M. Monthioux and L. Noé, Sub-Kelvin transport spectroscopy of fullerene peapod quantum dots, *Appl. Phys. Lett*., **89**, 233118/1–3 (2006).
[172] A. Eliasen, J. Paaske, K. Flensberg, S. Smerat, M. Leijnse, M.R. Wegewijs, H.I. Jorgensen, M. Monthioux and J. Nygard, Transport via coupled states in a C_{60} peapod quantum dot, *Phys. Rev. B*, **81**, 155431/1–5 (2010).
[173] E.L. Sceats and J.C. Green, Noncovalent interactions between organometallic metallocene complexes and single-walled carbon nanotubes, *J. Chem. Phys*., **125**, 154704/1–12 (2006).
[174] J. Sloan, R. Carter, R.R. Meyer, A. Vlandas, A.I. Kirkland, P.J.D. Lindan, G. Lin, J. Harding and J.L. Hutchison, Structural correlation of band-gap modifications induced in mercury

telluride by dimensional constraint in single walled carbon nanotubes, *Phys. Stat. Sol. (b)*, **243**, 3257–3262 (2006).
[175] C. Yam, C. Ma, X. Wang and G. Chen, Electronic structure and charge distribution of potassium iodide intercalated single-walled carbon nanotubes, *Appl. Phys. Lett*., **85**, 4484–4486 (2004).
[176] E.L. Sceats, J.C. Green and S. Reich, Theoretical study of the molecular and electronic structure of one-dimensional crystals of potassium iodide and composites formed upon intercalation in single-walled carbon nanotubes, *Phys. Rev. B*, **73**, 125441/1–11 (2006).
[177] K.V. Christ and H.R. Sadeghpour, Energy dispersion in graphene and carbon nanotubes and molecular encapsulation in nanotubes, *Phys. Rev. B*, **75**, 195418/1–7 (2007).
[178] C.Z. Loebick, M. Majewska, F. Ren, G.L. Haller and L.D. Pfefferle, Fabrication of discrete nanosized cobalt particles encapsulated inside single-walled carbon nanotubes, *J. Phys. Chem. C*, **114**, 11092–11097 (2010).
[179] J.-P. Cleuziou, W. Wernsdorfer, T. Ondarçuhu and M. Monthioux, Electrical detection of individual magnetic nanoparticles encapsulated in carbon nanotubes, *ACS Nano*, **5**, 2348–2355 (2011).
[180] R. Kozhuharova, M. Ritschel, D. Elefant, A. Graff, A. Leonhardt, I. Mönch, T. Mühl, S. Groudeva-Zotova, C.M. Schneider, Well-aligned Co-filled carbon nanotubes: preparation and magnetic properties, *Appl. Surf. Sci*., **238**, 355–359 (2004).
[181] D.S. Scholl and J.K. Johnson, Making high flux membranes with carbon nanotubes, *Science*, **312**, 1003–1004 (2006).
[182] A.I. Skoulidas, D.S. Scholl and J.K. Johnson, Adsorption and diffusion of carbon dioxide and nitrogen through single-walled carbon nanotube membranes, *J. Chem. Phys*., **124**, 054708/1–7 (2006).
[183] S. Kim, J.R. Jinscheck, H. Chen, D.S. Johnson and E. Marand, Scalable fabrication of carbon nanotube/polymer composite membranes for high flux gas transport, *Nano Lett*., **7**, 2806–2811 (2006).
[184] B.J. Hinds, N. Chopra, T. Rantell, R. Andrews, V. Gavalas and L.G. Bachas, Aligned multiwalled carbon nanotube membranes, *Science*, **303**, 62–65 (2004).
[185] K. Holt, H.G. Park, Y. Wang, M. Stadermann, A.B. Artyukhin, C.P. Grigoropoulos, A. Noy and O. Bakajin, *Science*, **312**, 1034–1037 (2006).
[186] A.I. Skoulidas, D.M. Ackerman, D.S. Scholl and J.K. Johnson, Rapid transport of gases in carbon nanotubes, *Phys. Rev. Lett*., **89**, 185901/1–4 (2002).
[187] H. Chen, J.K. Johnson and D.S. Scholl, Transport of diffusion is rapid in flexible carbon nanotubes, *J. Phys. Chem. B*, **110**, 1971–1975 (2006).
[188] M. Ouyang, J.-L. Huang and C.M. Lieber, Fundamental electronic properties and applications of single-walled carbon nanotubes, *Accts. Chem. Res.*, **35**, 1018–1025 (2002).
[189] A. Leonhardt, I. Mönch, A. Meye, S. Hampel and B. Büchner, Synthesis of ferromagnetic filled carbon nanotubes and their biomedical applications, *Adv. Sci. Tech*., **49**, 74–78 (2006).
[190] F. Yang, J. Hu, D. Yang, J. Long, G. Luo, C. Jin, X. Yu, J. Xu, C. Wang, Q. Ni and D. Fu, Pilot study of targeting magnetic carbon nanotubes to lymph nodes, *Nanomedicine*, **4**, 317–330 (2009).
[191] S. Hampel, D. Kunze, D. Haase, K. Krämer, M. Rauschenbach, M. Ritschel, A. Leonhardt, J. Thomas, S. Oswald, V. Hoffmann and B. Büchner, Carbon nanotubes filled with a chemotherapeutic agent: a nanocarrier mediates inhibition of tumor cell growth, *Nanomedicine*, **3**, 175–180 (2008).
[192] M. Arlt, D. Haase, S. Hampel, S. Oswald, A. Bachmatiuk, R. Klingeler, R. Schulze, M. Ritschel, A. Leonhardt, S. Fuessel, B. Büchner, K. Kraemer and M.P Wirth, Delivery of carboplatin by carbon-based nanocontainers mediates increased cancer cell death, *Nanotechnology*, **21**, 335101/1–9 (2010).
[193] C. Tripisciano, S. Costa, R.J. Kalenczuk and E. Borowiak-Palen, Cisplatin filled multiwalled carbon nanotubes – a novel molecular hybrid of anticancer drug container, *The Eur. Phys. J. B*, **75**, 141–146 (2010).
[194] B. Sitharaman, K.R. Kissell, K.B. Hartman, L.A. Tran, A. Baikalov, I. Rusakova, Y. Sun, H.A. Khant, S.J. Ludtke, W. Chiu, S. Laus, É. Tóth, L. Helm, A.E. Merbach and L.J. Wilson,

Superparamagnetic gadonanotubes are high-performance MRI contrast agents, *Chem. Commun*., 3915–3917 (2005).
[195] J.H. Choi, F.T. Nguyen, P.W. Barone, D.A. Heller, A.E. Moll, D. Patel, S.A. Boppart and M.S. Strano, Multimodal biomedical imaging with asymmetric single-walled carbon nanotube/iron oxide nanoparticle complexes, *Nano Lett.*, **7**, 861–867 (2007).
[196] S. Koyama, H. Haniu, K. Osaka, H. Koyama, N. Kuroiwa, M. Endo, Y.A. Kim and T. Hayashi, Medical application of carbon-nanotube-filled nanocomposites: The microcatheter, *Small*, **2**, 1406–1411 (2006).
[197] P. Kohli and C.R. Martin, Template-synthesized nanotubes for bionanotechnology and medicine, *J. Drug Deliv. Sci. Tech*., **15**, 49–57 (2005).
[198] H.J. Hwang, K.H. Byun and J.W. Kang, Carbon nanotubes as nanopipette: modelling and simulations, *Physica E*, **23**, 208–216 (2004).
[199] R. Singhal, Z. Orynbayeva, R.V.K. Sundaram, J.J. Niu, S. Bhattacharyya, E.A. Vitol, M.G. Schrlau, E.S. Papazoglou, G. Friedman and Y. Gogotsi, Multifunctional carbon-nanotube cellular endoscopes, *Nature Nanotechnol*., **6**, 57–64 (2011).
[200] L. Liao, J.C. Li, C. Liu, Z. Xu, W.L. Wang, S. Liu, X.D. Bai and E.G. Wang, Field emission of GaN-filled carbon nanotubes: High and stable emission current, *J. Nanosci. Nanotech*., **7**, 1080–1083 (2007).
[201] C.Y. Zhi, D.Y. Zhong and E.G. Wang, GaN-filled carbon nanotubes: synthesis and photoluminescence, *Chem. Phys. Lett*., **381**, 715–719 (2003).
[202] G.A. Domrachev, A.M. Ob'edkov, B.S. Kaverin, A.A. Zaitsev, S.N. Titova, A.I. Kirillov, A.S. Strahkov, S.Y. Ketkov, E.G. Domracheva, K.B. Zhogova, M.V. Kruglova, D.O. Filatov, S.S. Bukalov, L.A. Mikhalitsyn and L.A. Leites, MOCVD synthesis of germanium filled "diamond-like" carbon nanotubes from organo-germanium precursors and their field emission properties, *Chem. Vap. Dep*., **12**, 357–363 (2006).
[203] C. Yang, L.G. Yu, M.S. Wang, Q.F. Zhang and J.L. Wu, Low-Field Emission from iron oxide-filled carbon nanotube arrays, *Chin. Phys. Lett*., **22**, 911–914 (2005).
[204] G. Che, B.B. Lakshmi, C.R. Martin and E.R. Fisher, Metal-nanocluster-filled carbon nanotubes: Catalytic properties and possible applications in electrochemical energy storage and production, *Langmuir*, **15**, 750–758 (1998).
[205] X. Pan, Z. Fan, W. Chen, Y. Ding, H. Luo and X. Bao, Enhanced ethanol production inside carbon-nanotube reactors containing catalytic particles, *Nature Mater*., **6**, 507–511 (2007).
[206] G. Lota, E. Frackowiak, J. Mittal and M. Monthioux, High performance supercapacitor from hybrid-nanotube-based electrodes, *Chem. Phys. Lett*., **483**, 73–77 (2007).
[207] D.Y. Lu, Y. Li, S.V. Rotkin, U. Ravaioli and K. Schulten, Finite-size effect and wall polarization in a carbon nanotube channel, *Nano Lett*., **4**, 2383–2387 (2004).
[208] B. Corzilius, A. Gembus, N. Weiden, K.-P. Dinse and K. Hata, EPR characterization of catalyst-free SWNT and N@C_{60}-based peapods, *Phys. Stat. Solid*., **243**, 3273–3276 (2006).
[209] S.C. Benjamin, A. Ardavan, G.A.D. Briggs, D.A. Britz, D. Gunlycke, J. Jefferson, M.A.G. Jones, D.F. Leigh, B.W. Lovett, A.N. Khlobystov, S.A. Lyon, S.A. Morton, K. Porfyrakis, M.R. Sambrook and A.M. Tyryshkin, Towards a fullerene-based quantum computer, *J. Phys. Cond. Mat.*, **18**, S867–S883 (2006).